# Sediment Connectivity: A Framework for Analyzing Coastal Sediment Transport Pathways

**Stuart G. Pearson[1,2], Bram C. van Prooijen[1], Edwin P.L. Elias[2], Sean Vitousek[3], and Zheng Bing Wang[2,1]**

[1]Faculty of Civil Engineering and Geosciences, Delft University of Technology, PO Box 5048, 2600GA Delft, the Netherlands

[2]Deltares, P.O. Box 177, 2600MH Delft, the Netherlands

[3]Pacific Coastal and Marine Science Center, U.S. Geological Survey, Santa Cruz, California, USA

**Key Points:**

- Connectivity schematizes sediment transport pathways as a directed graph (series of nodes & links)
- Existing techniques in graph theory and network analysis can characterize complex coastal systems
- Example of Ameland Inlet demonstrates usefulness of connectivity in real-world applications

Corresponding author: Stuart G. Pearson, `s.g.pearson@tudelft.nl`

## Abstract

Connectivity provides a framework for analyzing coastal sediment transport pathways, building on conceptual advances in graph theory from other scientific disciplines. Connectivity schematizes sediment pathways as a directed graph (i.e., a set of nodes and links). Existing techniques in graph theory and network analysis provide a low barrier to entry for using connectivity to quantify complex coastal systems, exemplified here using Ameland Inlet in the Netherlands. We divide the study site into geomorphic cells (i.e., nodes), and then quantify sediment transport between these cells (i.e., links) using a numerical model. The system of cells and fluxes between them are then schematized in a network described by an adjacency matrix. Network metrics like link density, asymmetry, and modularity quantify system-wide connectivity. The degree, strength, and centrality of individual nodes identify key locations and pathways through the system. These metrics allow us to address fundamental questions about sediment bypassing of Ameland Inlet and the optimal placement of sand nourishments. Connectivity thus provides a novel and valuable technique for predicting the response of our coasts to climate change and the human adaptations it provokes.



## Plain Language Summary

The pathways that sand takes as it moves along coasts and estuaries are determined by a complex combination of waves, tides, geology, and other environmental or human factors. These pathways can be challenging to analyze and predict using existing approaches, so we turn to the concept of connectivity. Connectivity represents the pathways that sediment takes as a series of nodes and links, much like in a subway or metro map. This approach is well-used in other scientific fields, meaning that there are already numerous techniques available for us to apply towards solving coastal problems. To demonstrate the sediment connectivity approach, we use it to map sediment pathways at a coastal site in the Netherlands. The statistics computed using connectivity let us quantify and visualize these sediment pathways, revealing new insights into the coastal system. We can also use this approach to address practical engineering questions, such as where to place sand nourishments for coastal protection. Sediment connectivity thus provides a novel and valuable technique for predicting the response of our coasts to climate change and the human adaptations it provokes.

# 1 Introduction

## 1.1 Challenges Posed by Coastal Sediment Transport

Coasts and estuaries are complex geomorphic systems formed by connected fluxes of water and sediment. Tides, wind, and waves steer the development of coastal systems, and non-linear transport processes shape them. Tight feedback loops between morphology and hydrodynamic processes lead to dynamic landscapes in a wide range of coastal environments, from sandy beaches [*Masselink et al.*, 2006] to coral atolls [*Barry et al.*, 2007] or mudflats [*Friedrichs*, 2012]. Sediment transport pathways become particularly dynamic and convoluted in the vicinity of tidal inlets or estuaries [*Oertel*, 1972; *Hayes*, 1980; *Sha*, 1989; *Kana et al.*, 1999; *Elias et al.*, 2006; *Barnard et al.*, 2013a]. Sediment may be exchanged between the lagoon or estuary and the adjacent coastlines. For example, it may bypass the inlet via bar migration on an outer (ebb-tidal) delta [*FitzGerald*, 1982; *Sexton and Hayes*, 1983; *Gaudiano and Kana*, 2001; *Elias et al.*, 2019] or recirculate at the mouth [*Smith and FitzGerald*, 1994; *Hicks et al.*, 1999; *Son et al.*, 2011; *Herrling and Winter*, 2018]. The net import or export of sediment through the inlet system and changes to the ebb-tidal delta can have a profound influence on the morphological evolution of the adjacent coastline [*FitzGerald*, 1984; *Elias and Van Der Spek*, 2006; *Ranasinghe et al.*, 2012; *Hansen et al.*, 2013].

Effective management of coastal sediment is vital for sustainable protection against flooding and erosion [*Mulder et al.*, 2011; *Hanley et al.*, 2014; *Van Wesenbeeck et al.*, 2014]. In order to reliably predict coastal evolution, improved understanding of sediment flux pathways is necessary at multiple scales [*Ruggiero et al.*, 2016; *Vitousek et al.*, 2017]. Interruptions to the flow of sediment may degrade coastal systems, causing socioeconomic and ecological damage [*Roelvink*, 2015]. Furthermore, human interventions such as nourishments, protective structures, or basin closures can also affect coastal sediment transport pathways by interrupting existing paths, or by creating new ones [*Davis and Barnard*, 2000; *Fontolan et al.*, 2007; *Elias et al.*, 2012; *Eelkema et al.*, 2013; *Luijendijk et al.*, 2017; *Wang et al.*, 2015, 2018]. Understanding how human interventions change sediment pathways is important for gauging the effectiveness of the intervention, predicting potential consequences of that intervention, or assessing its environmental impact.

Where does the sediment from a given location go to? Furthermore, where does the sediment at that same location come from? These two questions are the most fun-

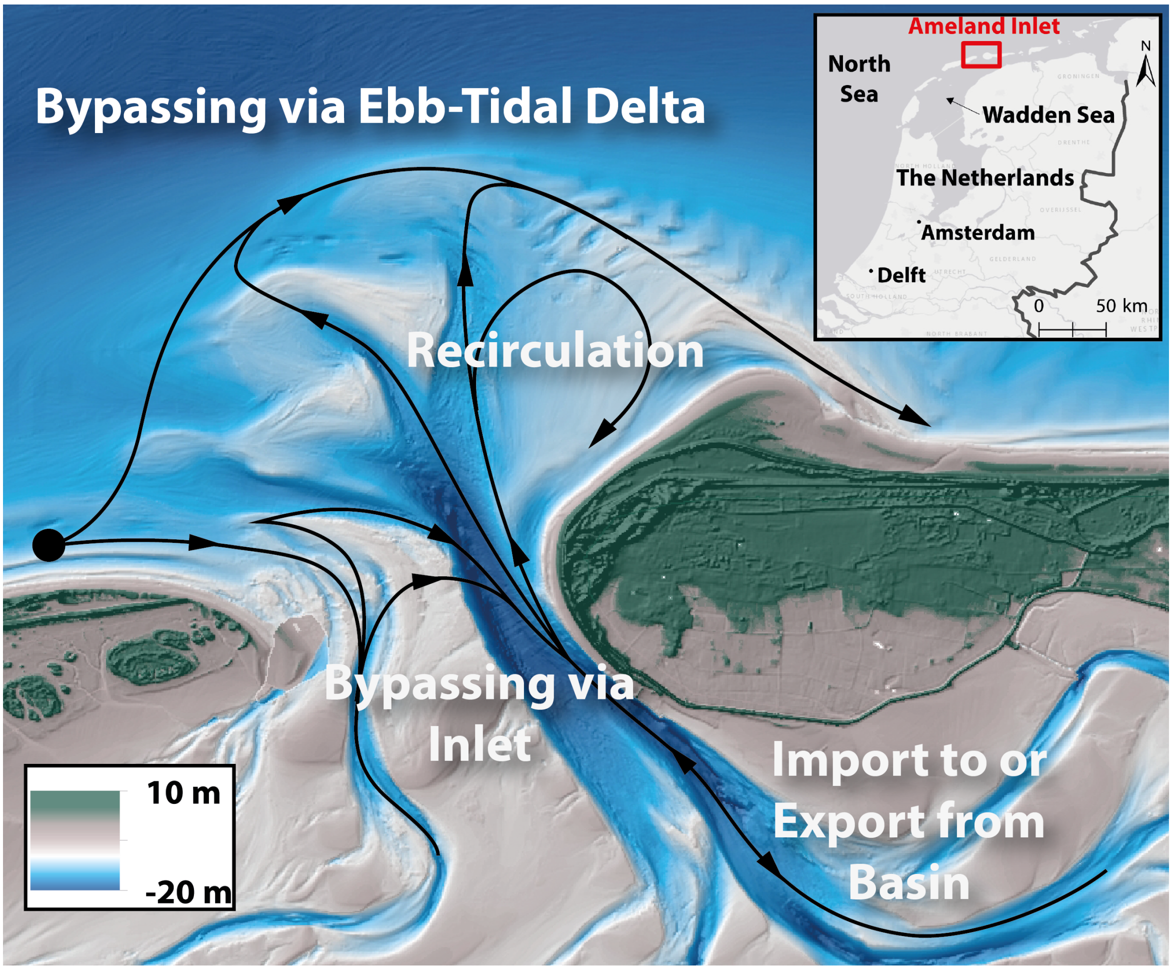


**Figure 1.** Conceptual diagram identifying key questions about sediment transport pathways, using Ameland Inlet in the Netherlands as an example. 1. Via which pathways does sediment bypass the inlet? 2. Is there a net import or export of sediment to/from the basin? From which sources? 3. Are there strong recirculations or opposing gross transports, or are transports largely unidirectional? 4. Where is the optimal location for a sand nourishment? 5. How do these paths change with grain size? 6. Can the domain be grouped into distinct sediment-sharing cells? Note that the modelling example presented in this paper only resolves sediment transport due to tidal flows, and neglects wave-driven transports. Bathymetry & topography source: Rijkswaterstaat.

damental to sediment transport. Yet rarely, if ever, are answers to these questions available, owing to the complexity of coastal sediment transport dynamics. Numerical models begin to answer these questions: at a given location, sediment goes to and comes from neighbouring grid cells over a single timestep. However, sediment transport pathways over large spatiotemporal scales are observed. Hence, the framework of sediment connectivity is critical to bridging the gap between connections among neighbouring regions to system-wide connections.

### 1.2 Connectivity: A Transformative Concept

In its most general sense, connectivity is a framework for representing the connections and flows between the different parts of a system. It has been widely adopted in other fields such as neurology [*Honey et al.*, 2007; *Rubinov and Sporns*, 2010], biology [*Maslov and Sneppen*, 2002], epidemiology [*Read et al.*, 2008], computer science [*Bassett et al.*, 2010]), transportation [*Derrible and Kennedy*, 2009; *Sperry et al.*, 2017], ecology [*Cantwell and Forman*, 1993; *Urban et al.*, 2009], and sociology [*Scott*, 2011; *Krause et al.*, 2007]. Connectivity has proven itself to be a transformative concept for describing and understanding complex dynamic systems in these disciplines [*Turnbull et al.*, 2018]. *Wohl et al.* [2019] identifies the value of connectivity in geomorphology, since it can illuminate interactions between seemingly-disparate and/or distant components of a system. *Keesstra et al.* [2018] argue that connectivity is useful for designing better measurement and modelling schemes for water and sediment dynamics.

Increasing attention has been paid to the topic of sediment connectivity in recent years, with 211 publications in the Web of Science explicitly mentioning "sediment connectivity in their titles, abstract, or keywords as of January 9th, 2020 (Figure 2). Although the number of publications mentioning "sediment connectivity" has increased exponentially (doubling every 4.75 years) since the beginning of the 21st century, the concept has seen limited application in coastal contexts. To our knowledge, none of these papers have sought to develop a unified framework (based on graph theory) to analyze coastal sediment transport. On the other hand, advances made in non-coastal fields like neurology and hillslope geomorphology have led to the development of techniques for assessing connectivity using graph theory and network analysis [*Newman*, 2003; *Csárdi and Nepusz*, 2006; *Rubinov and Sporns*, 2010; *Phillips et al.*, 2015; *Franz et al.*, 2016].

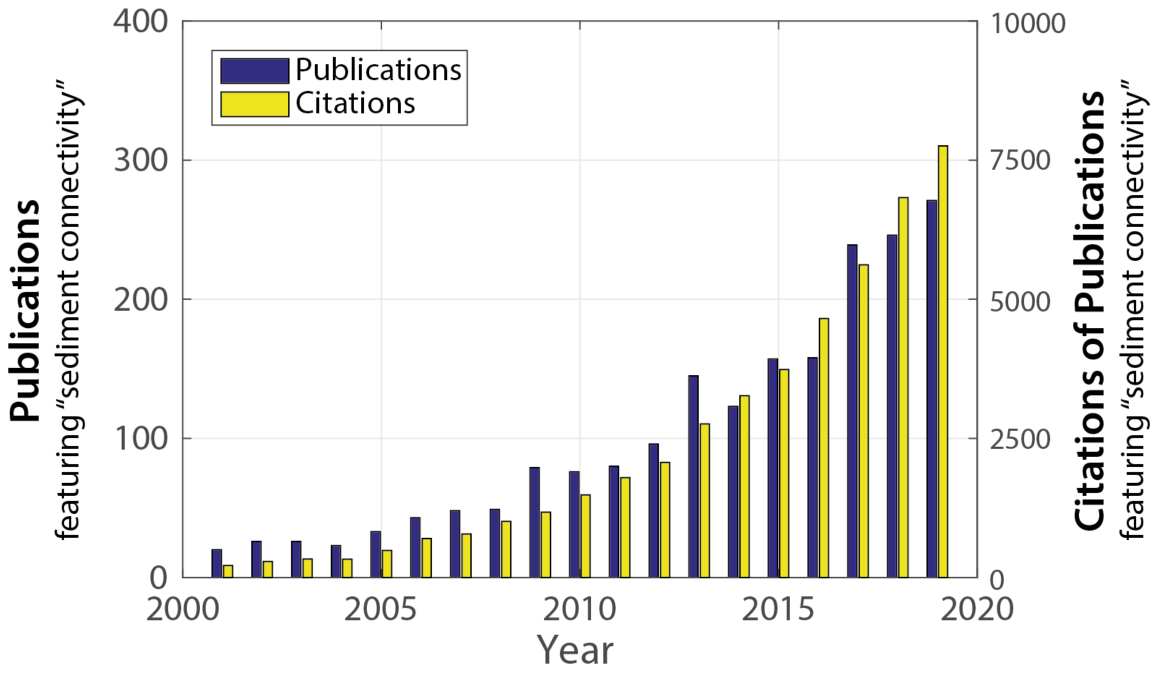


**Figure 2.** Number of publications in the Web of Science explicitly mentioning "sediment connectivity" in their titles, abstract, or keywords (search performed January 9th, 2020). Research on sediment connectivity has grown exponentially in popularity among geoscientists since 2000 (doubling approximately every 4 to 5 years), and yet has received limited attention in coastal contexts.

The major advance in connectivity analysis in recent years has been the adoption of techniques from network science. Within network science, graph theory conceptualizes a complex system as a series of nodes and the links between them, referred to as a network graph [*Newman*, 2003; *Phillips et al.*, 2015]. It provides a strong mathematical framework for analyzing geomorphic systems and quantifying sediment connectivity [*Heckmann and Schwanghart*, 2013]. With this approach, sources and receptors of sediment are defined as a series of $n$ nodes interconnected by $m$ links (Figure 3b). These links can have both magnitude (i.e., a weighted network) and direction (i.e., a directed network). They can represent fluxes between nodes (e.g., sediment transport rates) or some other spatial relationship (e.g., distance).

Nodes and links can be compiled into an $n \times n$ adjacency matrix, $A_{ij}$, with sources $i$ and receptors $j$ (Figure 3b). The matrix entry at $ij$ indicates the presence or absence of a connection (1 or 0, respectively), or alternatively, the magnitude of the flux. The adjacency matrix lies at the heart of network analysis, since many different algebraic techniques can be used applied to it. In this form, there are numerous statistical and algebraic techniques available for analyzing and interpreting the network [*Newman*, 2003; *Rubinov and Sporns*, 2010; *Phillips et al.*, 2015]. Furthermore, connectivity is a relatively accessible technique, as numerous open-source software libraries and packages are already available (e.g., iGraph [*Csárdi and Nepusz*, 2006], the Brain Connectivity Toolbox [*Rubinov and Sporns*, 2010], and Cytoscape [*Franz et al.*, 2016]).

Within geomorphology, the use of graph theory for analyzing connectivity has grown in popularity [*Heckmann et al.*, 2014; *Phillips et al.*, 2015; *Heckmann et al.*, 2018], for applications including sediment delivery in catchments [*Heckmann and Schwanghart*, 2013; *Cossart et al.*, 2018] and the development of sand bars in rivers [*Koohafkan and Gibson*, 2018]. Graph theory has also been effectively used for studying channel networks in river deltas [*Tejedor et al.*, 2015a,b, 2016, 2017; *Passalacqua*, 2017; *Hiatt et al.*, 2019].

A key strength of graph theory is the assessment of sediment cascades, the succession of different pathways linking nodes that may not be directly linked [*Heckmann and Schwanghart*, 2013]. This permits analysis of all possible sources contributing to a given location, as well as all possible receptors for sediment originating there. Graph theory provides a mathematical means of identifying and quantifying the structure of these individual connections in the context of a larger network [*Newman*, 2003]. Furthermore,

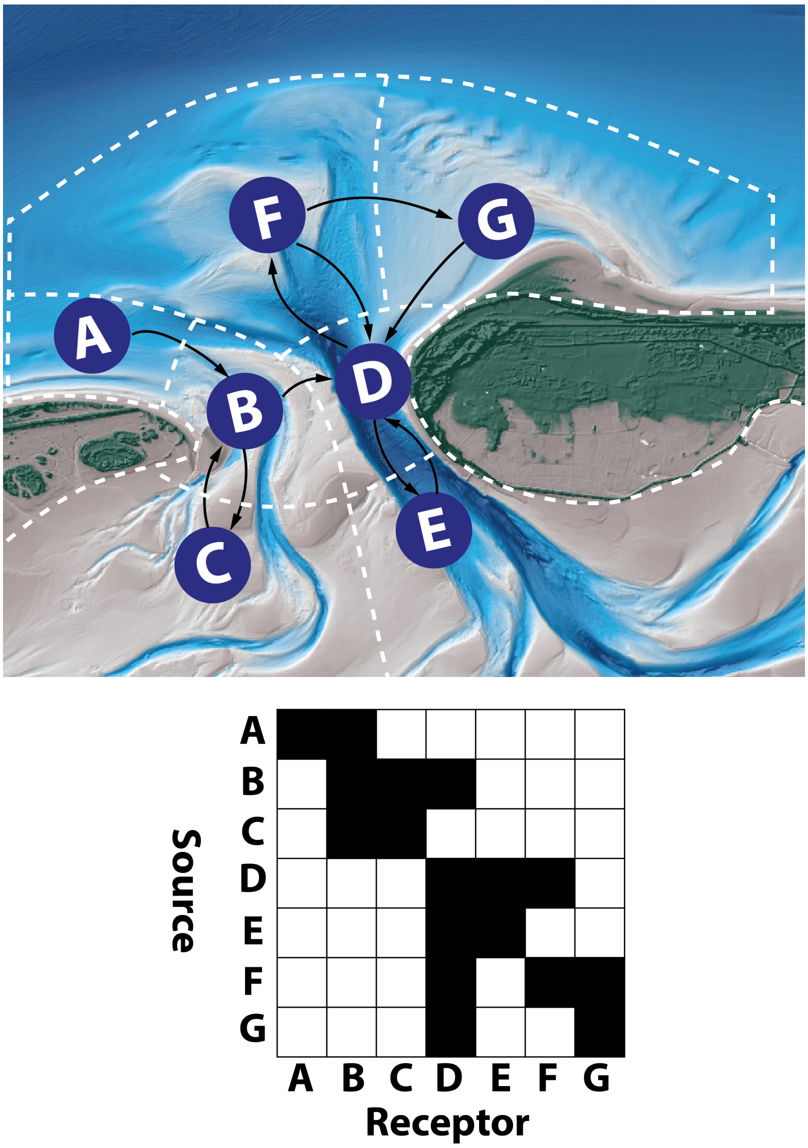


**Figure 3.** Conceptual diagrams explaining how graph theory can be used to quantify sediment connectivity. (a) Hypothetical sediment pathways at Ameland inlet, represented as an unweighted, directed network diagram. Blue nodes (A-G) are representative of the geomorphic cells defined with white dashed borders. Black arrows represent links or fluxes between the nodes. (b) An adjacency matrix $A$, the algebraic representation of the network graph presented in (a). Black squares indicate the existence of a pathway from a given source node $i$ to a given receptor node $j$. For instance, row B shows that node B acts as a source for nodes C and D, while column B shows that node B receives sediment from node A and node C. The main diagonal of the matrix corresponds to self-self connections, i.e., sediment that stays in or returns to the node where it originated.

assessing connectivity in this way can reveal emergent patterns not evident in other approaches (e.g., *Rossi et al.* [2014]), such as sediment transport vector fields produced from numerical models.

In spite of its widespread adoption for connectivity studies, graph theory has its limitations. Chiefly, delineating complex natural systems into a limited number of nodes, patches, or cells requires simplifications which can lead to a significant loss of information [*Moilanen*, 2011]. Thus, the initial schematization of a network is a step requiring careful attention and scrutiny, in order to ensure that important signals and patterns are not oversimplified.

Schematizing open coastal systems (i.e., without clearly delineated channels like those in river catchments or deltas) into networks is non-trivial. Nonetheless, graph theory has been embraced for connectivity analysis by the marine ecology and physical oceanography communities, primarily for analyzing larval dispersal, planning marine reserves, or quantifying the spread of pollutants [*Treml et al.*, 2008; *Cowen and Sponaugle*, 2009; *Grober-Dunsmore et al.*, 2009; *Gillanders et al.*, 2012; *Burgess et al.*, 2013; *Kool et al.*, 2013; *Paris et al.*, 2013; *Rossi et al.*, 2014; *Rogers et al.*, 2016; *Storlazzi et al.*, 2017; *Hock et al.*, 2017; *Condie et al.*, 2018; *van Sebille et al.*, 2018]. Since graph theory has already proven its usefulness for describing transport processes in marine environments, it is therefore also well-suited to analyzing sediment connectivity there.

### 1.3 Objectives & Outline

The objective of this study is to demonstrate that connectivity is a useful framework for understanding sediment transport pathways in coastal environments and solving related sediment management problems. We summarize the relevant advances in connectivity analysis made in other fields and highlight their utility for coastal applications. The remainder of this paper is presented in four sections. In the following section, we lay out a general methodology for applying connectivity (Section 2). To demonstrate the use of connectivity in coastal settings, we apply the concept to a case study of Ameland Inlet in the Netherlands (Section 3). We then discuss the utility and limitations of this approach, and provide an outlook for future research into how connectivity might be further adapted and improved for use in coastal environments (Section 4 & 5).

# 2 Methodology

We consider three main steps in order to apply connectivity to a coastal system:

1. **Defining connectivity**: what is the fundamental unit of connectivity, and are we concerned with structural or functional connectivity?
2. **Developing a network**: how can available data or model output be schematized in a network?
3. **Analyzing connectivity**: how can we measure the connectivity and emergent patterns of a network at different scales?

Answering these questions provides a framework with which connectivity can be assessed for coastal systems.

## 2.1 Defining Connectivity

### *2.1.1 Fundamental Units*

In order for the concept of connectivity to be applied, we must first define the entities or *fundamental units* between which connections exist. In neurological connectivity, the fundamental unit could be neurons or different parts of the brain, and in social networks it could be an individual person [*Turnbull et al.*, 2018]. Ecologists often use the concept of the *habitat patch* [*Calabrese and Fagan*, 2004] or ecosystem [*Turnbull et al.*, 2018]. For geomorphological applications, *Poeppl and Parsons* [2018] propose the concept of the geomorphic cell as the fundamental unit of connectivity. Within a geomorphic cell, morphology and sediment transport processes remain relatively uniform.

Known sources and sinks of sediment (e.g., sea cliffs or submarine canyons) or criteria like depth, sediment transport patterns, or morphological characteristics can be used to define these cells (e.g., *Jeuken and Wang* [2010]; *Stive et al.* [1998]; *Stive and Wang* [2003]; *Lodder et al.* [2019]). Geomorphic cells can also be derived using digital terrain model (DTM) cells as a basis [*Heckmann et al.*, 2014], although *Poeppl and Parsons* [2018] discourage the "thoughtless adoption of DTM cells at whatever resolution happens to be available", since those cells do not necessarily have a meaningful relationship to the sediment transport within them. If no information about sediment fluxes is known *a priori*, then expert judgment may be used for identifying appropriate geomorphic cells.

The spatial definition of geomorphic cells depends on the timescale under consideration. Regions delineated as geomorphic cells based on morphological characteristics or relatively constant sediment and water fluxes may cease to be representative as the landscape evolves. For example, on a long enough timescale, a shallow shoal could develop in a cell originally defined as a deep channel. Thus the spatial scale of geomorphic cells can affect the connectivity observed in a given period [*Poeppl and Parsons*, 2018].

#### *2.1.2 Structural & Functional Connectivity*

Once the fundamental unit is defined, we must consider which type of connectivity is relevant: structural or functional. Structural connectivity concerns the spatial anatomy or form of the network (i.e., how the units are spatially arranged relative to one another), whereas functional connectivity concerns the dynamic fluxes passing within the network (e.g., how much material passes between cells).

Structural connectivity is often defined in terms of adjacency: two neighbouring units not separated by physical barriers are structurally connected. For example, we can consider an open tidal inlet and the adjacent sea, or a river channel and its tributary. However, just because two units are adjacent, does not mean that they will be functionally connected with fluxes between them. This is why it is important to distinguish between structural and functional connectivity.

Two units are functionally connected if there is some flux between them, such as sediment, water, or organisms. Units need not have strong structural connections to be functionally connected: fluxes may exist between adjacent units, but there may be teleconnections, wherein spatially remote cells can still influence one another (e.g., *Phillips et al.* [2015]). For functional connectivity, it is also necessary to define the dimensions and units of the fluxes under consideration (e.g., mass of sediment, number of particles, discharge, number of organisms in a given time period). Furthermore, functional connectivity can be derived using either Eulerian input (i.e., measured or modelled fluxes at fixed locations) or Lagrangian input (i.e., by tracking a given particle as it moves through the system [*van Sebille et al.*, 2018]. Consensus on how to definitively measure and quantify connectivity is currently lacking [*Wohl et al.*, 2019].

As with defining geomorphic cells, the inherent feedback between structural and functional connectivity complicates matters. Sufficient gradients in sediment fluxes will eventually modify the landscape or seascape, which will in turn modify the sediment fluxes. For example, high alongshore sediment transport can lead to the closure of a tidal inlet, which then disconnects the associated basin from the sea (e.g., *Duong et al.* [2016]). Morphodynamics are essentially the relationship between form and process, between structural and functional connectivity.

Functional connectivity has a temporal dimension [*Defne et al.*, 2016], and should thus be determined over a sufficiently long interval that areas of interest can be connected, but not so long that the structural connectivity changes. Spatial and temporal scales determine connectivity and vice versa. *Keesstra et al.* [2018] argue that structural connectivity has no temporal dimension, as it is a snapshot of the system's architecture at a given moment. This suggests that it would be better to adopt a morphostatic (fixed-bed) modelling approach, if the timescale of sediment fluxes is smaller than the timescale of observable morphologic change at the modelled spatial scale. This interdependency between structural and functional connectivity is still regarded as an intractable problem across the literature [*Turnbull et al.*, 2018; *Wohl et al.*, 2019].

Also important to consider is the notion of disconnectivity: the absence or removal of a given connection. Blockages in a system may inhibit sediment fluxes and thereby change the structural and functional connectivity of a given network [*Fryirs*, 2013]. Such disconnections may be natural (e.g., the closure of a seasonal tidal inlet) or anthropogenic (e.g., the construction of a storm surge barrier or tidal energy barrage across an estuary).

### 2.2 Developing a Network

Numerous qualitative and quantitative metrics have been developed to estimate connectivity [*Calabrese and Fagan*, 2004; *Kindlmann and Burel*, 2008; *Heckmann et al.*, 2018], but the most powerful means of quantifying connectivity is via graph theory [*Newman*, 2003; *Rubinov and Sporns*, 2010; *Phillips et al.*, 2015; *Heckmann et al.*, 2014]. To develop a network, geomorphic units can be represented as nodes, and the sediment fluxes or structural connections between them as links. Coastal sediment connectivity networks can be populated using field measurements, numerical model output, or a combination of the two. The possibility to integrate and compare multiple sources of data in a unified framework is an advantage of the connectivity approach.

Sediment transport can be estimated using Eulerian measurements at a single point, based on current velocities and suspended sediment concentrations (e.g., *Gartner et al.* [2001]; *Erikson et al.* [2013]). However, it is expensive and impractical to measure continuously for long periods of time at a sufficient number of points to reveal connectivity. While analyzing the differences between repeated bathymetric surveys can yield insight into the rates of morphological change (e.g., *Jaffe et al.* [1997]; *Elias et al.* [2012]), it does not give sufficient information to attribute directional transport.

Sediment tracer studies (both artificial [*Black et al.*, 2007; *Elias et al.*, 2011; *Bosnic et al.*, 2017] and natural [*Rosenbauer et al.*, 2013; *Hein et al.*, 2013; *McGann et al.*, 2013; *Wong et al.*, 2013; *Reimann et al.*, 2015]) offer a Lagrangian technique for identifying pathways, but are challenging to execute and recover *Elias et al.* [2011]. Grain trend analysis [*McLaren and Bowles*, 1985; *McLaren et al.*, 1998; *Duc et al.*, 2016; *McLaren*, 2013; *Gao and Collins*, 1991; *Le Roux and Rojas*, 2007; *Velegrakis et al.*, 2007; *Poizot et al.*, 2006, 2008] and analysis of bedform asymmetry [*Sha*, 1989; *Bartholdy et al.*, 2002; *Velegrakis et al.*, 2007; *Barnard et al.*, 2013a] offer additional techniques for identifying sediment pathways. However, field measurements alone are generally too limited to quantify sediment connections on the decadal timescales of typical interest for engineering and policy decisions.

As an alternative or complement to field measurements, numerical models provide a convenient way of inferring connectivity, since they can calculate fluxes at every point in a system [*Wohl et al.*, 2019]. The mean sediment transport vector field generated by a model can be used to visualize residual transport pathways (e.g., *Elias and Hansen* [2013]; *Herrling and Winter* [2014]; *Gelfenbaum et al.* [2017]). Alternatively, Lagrangian approaches to analyzing modelled sediment transport can be used. *Elias et al.* [2011], *Nienhuis and Ashton* [2016], and *Beck and Wang* [2019] used an approach where sediment originating from a particular location was labelled as a unique sediment class in a morphodynamic model, and then followed as it dispersed throughout the model domain.

Lagrangian particle tracking models (e.g., *MacDonald and Davies* [2007]; *Soulsby et al.* [2011]; *van Sebille et al.* [2018]) are also a useful tool for tracking sediment and defining transport pathways. One can either consider the final resting place of a given sediment particle at a given time (a depositional approach) or instead track the complete history of that particle. The disadvantage of a depositional approach to connectivity is that a pathway with zero transport gradient may be very well connected, and yet leave no trace of the sediment it is transporting [*Wohl et al.*, 2019]. For example, the main channel of a tidal inlet near morphological equilibrium may convey large volumes of sediment, but this sediment does not necessarily accumulate there, which would give the erroneous impression of low connectivity. Hence, the choices made in how sediment transports or particle trajectories are tabulated from numerical model output can significantly affect the conclusions drawn from connectivity analysis.

Once the data source has been chosen and organized into cells and fluxes, the network can be compiled. The contribution from a given source cell to every other possible receptor cell in the system constitutes one row of an adjacency matrix. By carrying out this calculation for each source in the system, we arrive at a fully-populated adjacency matrix representing all the sediment fluxes in our system (e.g., Figure 4g). Thus, these large and complex datasets can be reduced to a relatively simple form, all visualized as a network diagram (e.g., Figure 4a). Once the adjacency matrix has been defined, it can be analyzed using a variety of algebraic and statistical techniques.

### 2.3 Analyzing Connectivity

With the coastal system reduced to a adjacency matrix of sediment fluxes, we can begin to quantify and analyze connectivity. This is where connectivity has added value as a framework over existing approaches: an abundance of analytical metrics and statistics can be used once the data has been organized into a network. Here, we focus on a selection of connectivity metrics that lead to useful insights for coastal sediment management, both at a system level and for individual units.

#### *2.3.1 System Level*

System-level connectivity metrics are important to consider because in a complex network, the overall structure and connectivity will influence the connections between individual nodes at smaller scales.

**Link Density**

To gain insight into the overall connectivity of a given system, we can consider the link density ($D$), which is the number of connected links relative to the total number of possible links. If self-self connections are neglected, the maximum possible connections

$m_{max}$ is $(n^2 - n)$ for directed networks and $(n^2 - n)/2$ for undirected networks, where $n$ is the number of nodes in the network [*Phillips et al.*, 2015]. A fully open network is one in which each node is connected to every other node ($D = m/m_{max} = 1$). A system that is completely immobile or has only local circulation within a given node corresponds to a fully closed network, where none of the nodes are connected to any of the others ($D = m/m_{max} = 0$) [*Cowen and Sponaugle*, 2009]. In reality, most networks will lie somewhere in between (e.g., Figure 4a, with $D = 0.33$). Link density is a function of the observation or simulation time, since longer periods may allow sediment to travel greater distances and hence connect with additional receptors. This may be useful for comparing the general behaviour of a system at different time scales or in different scenarios.

**Asymmetry**

By definition, undirected networks have symmetric adjacency matrices. For directed networks like in Figure 4, asymmetry implies a net flux: more material is going to a given node than coming from it, or vice versa. Asymmetric connectivity is critical for predicting future morphological changes, since a net flux of sediment will lead to erosion or accretion at a given node.

Asymmetry can be revealed by decomposing an adjacency matrix $A$ into its symmetric $A_{sym}$ and skew-symmetric $A_{sk}$ components [*Kundu and Cohen*, 2008]:

$$A = A_{sym} + A_{sk} = \frac{1}{2}(A + A^T) + \frac{1}{2}(A - A^T) \quad (1)$$

Where $A^T$ is the transpose of the adjacency matrix. The skew-symmetric matrix $A_{sk}$ should directly correspond to the net sediment transport of a system, and the symmetric matrix $A_{sym}$ to the gross transports that cancel each other out. Decomposing a matrix in this way can be useful for understanding the transport pathways that drive morphological changes.

The degree of symmetry $s$ in the network can be summarized using the approach of *Esposito et al.* [2014]:

$$s = 1 - \frac{2}{n(n-1) - 2u} \sum_{i=1}^{n} \sum_{j=i+1}^{n} \frac{|A_{ij} - A_{ji}|}{A_{ij} + A_{ji}}$$

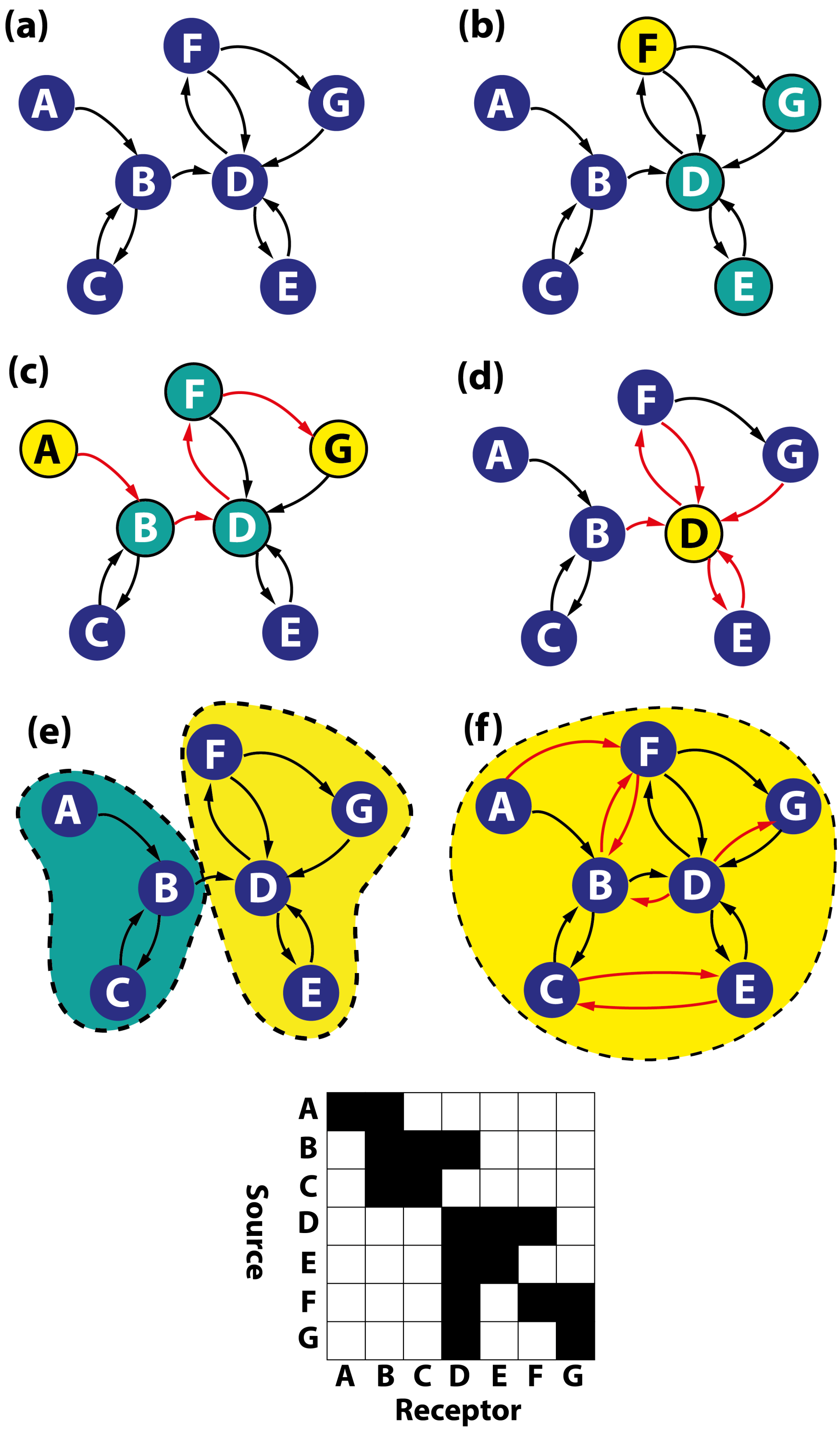


**Figure 4.** Examples of questions that can be answered via connectivity. (a) Simple unweighted directed network diagram from Figure 3(c); (b) What are the possible receptors for sediment from Source F? (c) What is the shortest pathway between A & G?; (d) Which node is the most interconnected (has the highest degree) in the system? (e) Can the system be easily separated into distinct modules? (yes); (f) If additional links are added, can the system still be easily separated into modules? (no). (g) Adjacency matrix for the simple network shown in (a-e).

$$= \quad 1 - \frac{2}{n(n-1) - 2u} \sum_{i=1}^{n} \sum_{j=i+1}^{n} \frac{|(A_{sk})_{ij}|}{(A_{sym})_{ij}} \tag{2}$$

Where $s$ is the symmetry index, $u$ is the number of completely unconnected node pairs ($A_{ij} = A_{ji} = 0$). When $s = 1$, the network is fully symmetric, and when $s = 0$, there are no reciprocated connections in the network (fully asymmetric).

**Modularity**

Modules or communities are densely-interconnected clusters of nodes with limited external connection. The degree to which a network can be be divided into such clusters is known as modularity, $Q$ [*Leicht and Newman*, 2008]:

$$Q = f_{mod} - f_{rnd} \tag{3}$$

Where $f_{mod}$ denotes the fraction of links within a module and $f_{rnd}$ denotes the expected fraction of such links based on random chance. These modules can be determined using a variety of cluster optimization techniques such as the Infomap [*Rossi et al.*, 2014] or Louvain [*Rubinov and Sporns*, 2010] algorithms.

Networks that can be clearly delineated into non-overlapping clusters have high modularity $Q > 0$ (Figure 4e), whereas networks with few coherent groups have low modularity $Q < 0$ (Figure 4f). For instance, *Rossi et al.* [2014] uses modularity to identify 'hydrodynamic provinces', regions that are internally well-connected but are poorly linked to each other. This procedure could be used to delineate geomorphic cells (as per *Poeppl and Parsons* [2018]) or to examine emergent behaviour. Such grouping may be the result of similarities in morphology, initial sediment distribution, or hydrodynamic forcing.

### *2.3.2 Individual Nodes & Links*

Graph theory also offers numerous metrics with which to gauge the influence of individual nodes and links in a network. These statistics may provide practical insights into the role of a given node or link in transmitting sediment, and identify key vulnerabilities in the system.

**Connectivity between Specific Nodes**

Most simply, a network can be directly queried to examine the connectivity between specific nodes or groups of nodes. For example, we see in Figure 4b that Node F is directly or indirectly a source for Nodes D, E, and G. However, there are no possible pathways leading from Node F to Node C. Hence, if this were a coastal sediment system where the goal was to eventually nourish Node C with sand, Node F would not be an optimal location. In another example, we can consider the shortest path between two nodes (e.g., Figure 4c), which may be useful for quantifying processes like inlet bypassing. Asymmetry of connections between individual nodes or specific groups of nodes may also provide useful insight into net transport patterns.

**Degree**

Degree quantifies the number of links connected to a given node. For directed networks, this can further be decomposed into an in-degree $k_{in}$ and an out-degree $k_{out}$ (Figure 4b). For example, Node D in Figure 4d has an in-degree of 4 and an out-degree of 2. Degree provides insight into the diversity of different sources or sinks that a given node has. A network's degree distribution ($P(k) = n_k/n$, where $n_k$ is the number of nodes of degree $k$ and $n$ is the total number of nodes in the network) can provide an indication of the overall network structure or topology [*Phillips et al.*, 2015]. If each node has a similar degree, the network will have a relatively uniform, distributed structure. However if the degree distribution is exponential, the network will be more centralized with a few dominant hubs or clusters. This relationship highlights how connectivity at the level of individual nodes can cascade upwards to shape connectivity at the overall system level.

**Strength**

Strength is the sum of all fluxes in and out of a given node for weighted networks, and can be computed directly from the adjacency matrix. For weighted, directed networks, this can be further decomposed into in-strength and out-strength. Nodes with a high in-strength are sinks, which is useful for identifying zones of sediment accumulation or convergence. Nodes with a high out-strength are sources, so material will tend to disperse there. Knowledge of these key nodes can inform dredging/nourishment strategies.

This may be more insightful than degree, since high degree does not necessarily equal high strength, especially where fluxes are unevenly distributed throughout the system. For example, even though Node D in Figure 4d has a higher in-degree than out-degree, if the out-strength is higher than in-strength, it will be a net source rather than net sink.

**Centrality**

Centrality quantifies how "central" a given node or link is within the context of the system as a whole. Betweenness centrality refers to the proportion of all paths in a network that pass through a given node or link [*Phillips et al.*, 2015]. Betweenness centrality $B$ is calculated based on the number of shortest paths that pass through each node, where the distance along paths is calculated in terms of inverse sediment flux between nodes ($d_{ij} = 1/A_{ij}$s). That is, nodes connected by large fluxes are considered closer together in the topology of the network, and nodes with weak connections are more distant, irrespective of actual geographic distances. Hence nodes with high betweenness centrality represent crucial nodes that may more efficiently transmit sediment through the rest of the system. This could translate to a greater vulnerability to disruptions, or could be used identify strategic locations for more dispersive nourishments. Thus, betweenness centrality gives more insight into the relationship between network structure as a whole and individual nodes than just degree or strength.

The comparison metrics in this section examine both the network structure as a whole and individual nodes or links. To illustrate their ease of application and usefulness in answering practical questions about coastal sediment systems, these metrics are applied to a case study of a Dutch tidal inlet in the following section.

## 3 Case Study: Ameland Inlet

To illustrate the principles and analysis techniques discussed in previous sections, we apply the sediment connectivity approach to Ameland Inlet, a tidal inlet located in the Netherlands (Figure 1). The safety of the Dutch coast against coastal flooding is directly linked to the volume of sand contained in its dunes and beaches, so there is a strong need for sediment management there *Hanson et al.* [2002]; *Stive et al.* [2013]. The beaches and shoreface are regularly nourished with sand, so connectivity provides an approach that can be used for optimizing those nourishments and improving our understanding of the underlying natural system.

Based on our general understanding of tidal inlets and our prior knowledge of Ameland, we can make a hypothesis about the system's connectivity. Connectivity of a given grain size class should depend on its mobility threshold, the energy available to transport it, and its initial spatial distribution. We thus expect higher connectivity for finer sand and lower connectivity for coarser sand. This is because the lower critical shear stress threshold for fine sand means that it will be more easily mobilized and transported longer distances. Conversely, the higher threshold for mobilization of coarse sediment means that only the most energetic conditions can transport it. In addition, fine sand has a wider initial spatial distribution in this model, whereas coarser sand is only found in the deepest channels (Figure 5).

We also expect higher connectivity in regions with greater hydrodynamic energy to mobilize sediment, like the main channels and ebb-tidal delta. Conversely, deeper areas offshore and calmer areas at the periphery of the inner basin are expected to have low connectivity. We also expect the main channels to function as transport bottlenecks, since they represent the only routes from the ocean to the inner basin (i.e., no transport through the islands in this model), whereas there are more possible pathways between different points on the ebb-tidal delta (e.g., *Herrling and Winter* [2018]).

To illustrate the coastal sediment connectivity framework, we used the Delft3D process-based numerical sediment transport model [*Lesser et al.*, 2004] to assess the fate of sediment as it moved between specific morphological units defined in the model domain. Delft3D has been widely used for simulating coastal sediment transport [*Elias et al.*, 2006; *Herrling and Winter*, 2014; *Nienhuis and Ashton*, 2016; *Huisman et al.*, 2018]. We used an existing Delft3D model [*de Fockert*, 2008; *Elias et al.*, 2015; *Wang et al.*, 2016; *Bak*, 2017] as a basis for this example. The model is 2D and represents a 40x30 km domain, with a maximum resolution of $\approx 80m$ (Figure 5). Data from the 2016 Vaklodingen survey [*Rijkswaterstaat*, 2016] was used to create the bathymetry.

The existing model was simplified to demonstrate the concepts of connectivity, featuring a schematized morphological tide (e.g., *Latteux* [1995]) at the offshore and seaward lateral boundaries. The lateral boundaries within the Wadden Sea are considered closed in these simulations. Ameland Inlet has a tidal range of between 1.5-3 m, and tidal prism of $400 - 500Mm^3$ [*Elias et al.*, 2019]. The eastward-propagating tide drive currents of approximately 1 m/s in the main channel of the inlet at ebb and flood. Waves and inter-basin wind-driven flows are known to be important processes for Ameland Inlet [*Duran-Matute et al.*, 2014; *Van Weerdenburg*, 2019; *Lenstra et al.*, 2019; *Elias et al.*, 2019; *Brakenhoff et al.*, 2019; *De Wit et al.*, 2019], but are neglected here for simplicity.

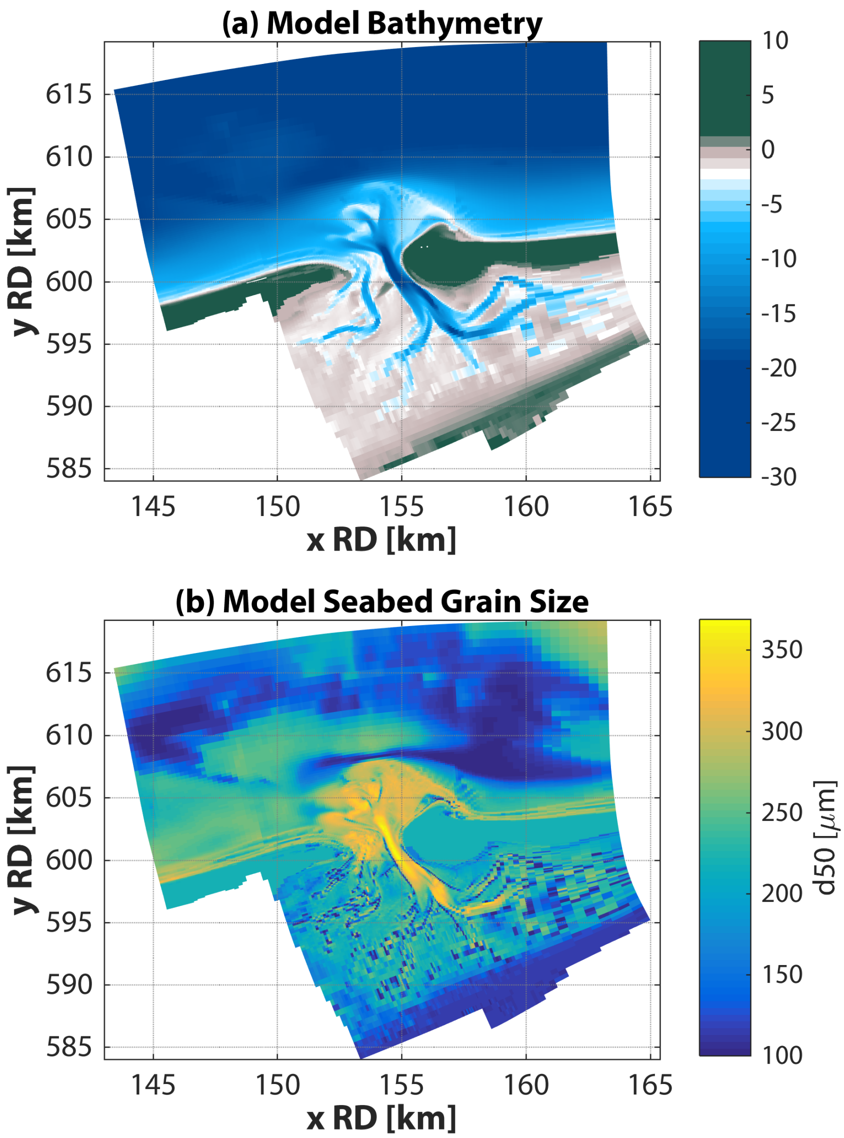


**Figure 5.** (a) Initial bathymetry of Delft3D numerical model used to calculate connectivity, based on *Rijkswaterstaat* [2016]. The maximum resolution of the grid is approximately 80 m at the inlet. (b) Initial sediment distribution in Delft3D model. Median grain size ($d_{50}$ [$\mu$m]). The coarsest sediment can be found in the deepest parts of the channel where tidal currents are strongest, whereas the finest sediment is located offshore, on intertidal flats inside the basin, and seaward of the ebb-tidal shoals.

Seabed sediment at Ameland Inlet is typically fine to medium sand, so four sediment grain size classes were chosen to simulate the influence of grain size variation (100, 200, 300, 400 $\mu$m). The sediment was initially distributed according to measured samples [*Rijkswaterstaat*, 1999], after which a bed composition generation run was carried out to redistribute the sediment in equilibrium with the model bathymetry, as per *Van Der Wegen et al.* [2011]. The model has a 12 hour spinup period, and an equilibrium concentration condition is specified at the boundaries. A transport layer thickness of $0.5m$ and maximum underlayer thickness of $1m$ are used to describe vertical variations in bed composition.

We adopted a morphostatic (fixed bed) modelling approach, but permitted sediment exchange between the bed and water column. We ran the model for 6 months (360 tidal cycles) with a morphological factor of 1. This ensures that the modelled timescale is smaller than the timescale of observable morphologic change at the chosen spatial scale, based on annual bathymetric surveys [*Elias et al.*, 2019]. This is also long enough to ensure that the network is well-connected with few separate subsystems or *components*.

This model output was used to populate a network, and then graph theory used to analyze connectivity at different space and time scales.

### 3.1 Defining Connectivity

For this example, we examine the functional connectivity of Ameland Inlet by looking at sediment fluxes between different parts of the system. To determine this functional connectivity, we started by defining 25 geomorphic cells, (Figure 6a). These cells were delineated subjectively on the basis of depth contours but also of their functionality. For instance, shallow parts of the ebb-tidal delta may occur at similar depths to the inner basin, but are morphologically distinct, with different hydrodynamic forcing and sediment composition. As such, the model domain was broken into offshore regions, ebb-tidal shoals, channels, beaches, and intertidal flats.

25 model simulations were prepared, one for each geomorphic cell (Figure 6b). In each simulation, a different cell served as the source node, and the remaining 24 cells were receptors. Similarly to *Elias et al.* [2011] and *Nienhuis and Ashton* [2016], we track the motion of sediment (and hence functional connectivity) from source to receptor by using a series of unique sediment classes. A total of eight sediment classes were included

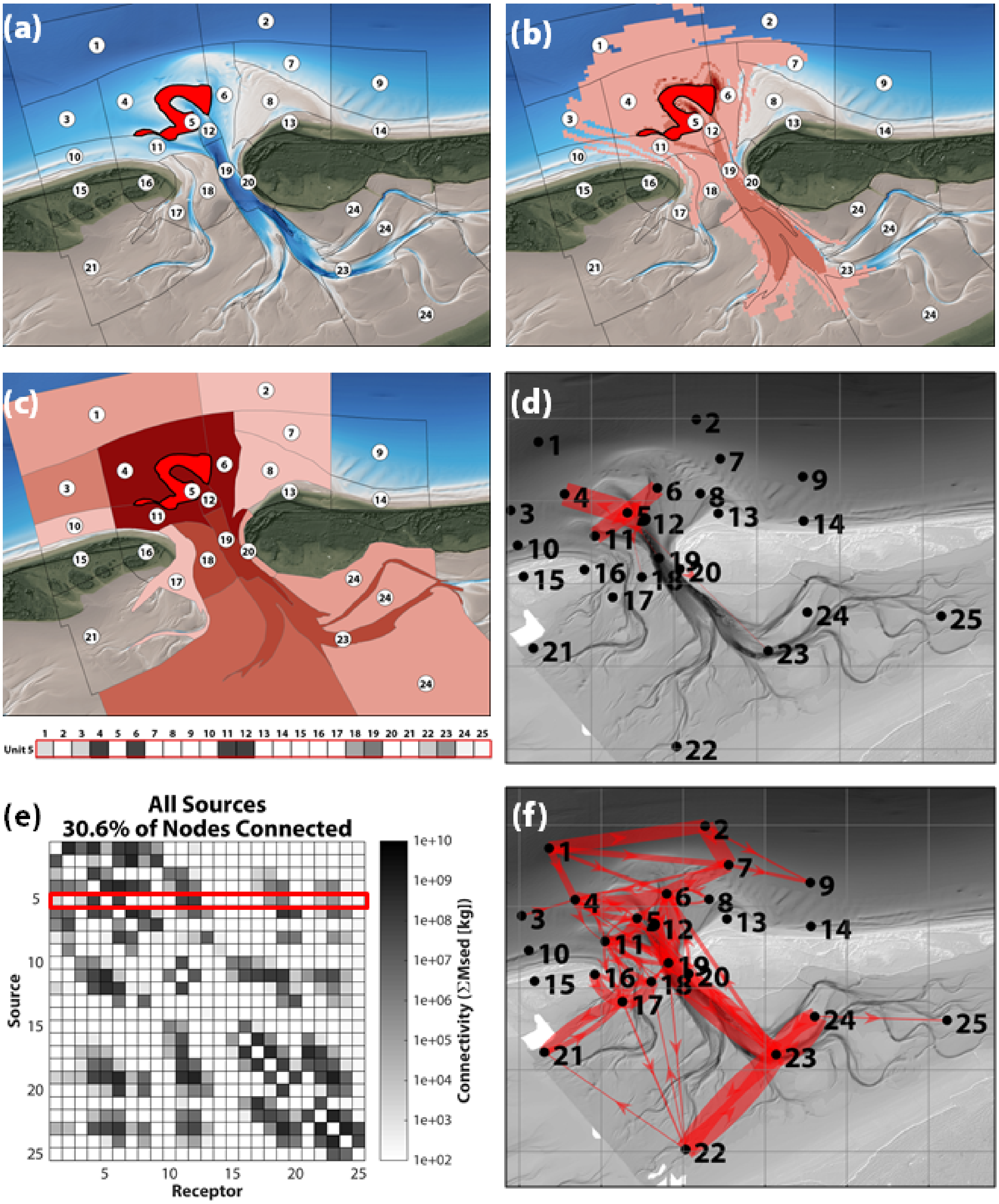


**Figure 6.** Connectivity methodology using process-based numerical model. Example using sediment from Node 5. (a) Step 1: Definition of source/receptor nodes (geomorphic cells) and labelling of tracer sediment classes. (b) Step 2: Running the model and tracking sediment. (c) Step 3. Tabulating the mass of tracer sediment from Node 5 to each other node, and compiling into one row of an adjacency matrix. (d) Example of a network based on sediment from Node 5 alone. (e) Adjacency matrix for full weighted, directed network with contribution from Unit 5 highlighted in red. (f) Network diagram for full network, where thicker links correspond to larger sediment fluxes. Only the top 10% of connections are shown here, in order to clarify the dominant patterns.

in the model: four "tracer" classes and four "background" classes. In each simulation, sediment within the source node was labelled as a tracer, while the sediment elsewhere in the model domain was labelled as "background" sediment. In this way, it is possible to track the movement of the tracer sediment and distinguish its fate from that of the surrounding sediment.

### 3.2 Developing a Network

Net fluxes of sediment determine the long-term morphological evolution, rather than the gross fluxes of sediment passing through a given cell on each tidal cycle. However, these gross fluxes are often much larger than the net fluxes. To measure the residual rather than gross fluxes (and avoid erroneously large or misleading trends), we record the mass of sediment in the bed and water column of a given cell at the end of an integer multiple of tidal cycles (Figure 6b). To limit the influence of numerical z (e.g., from rounding or truncation errors) and focus on pathways showing a clear signal, we apply a minimum threshold of 1000 kg per 6 months to all connections (up to 7 orders of magnitude smaller than the strongest fluxes). This represents an Eulerian definition of connectivity, in comparison to Lagrangian methods which would consider the full lifetime path of a given tracer particle.

The total mass of sediment from a given source in each receptor produces a single row of an adjacency matrix (see example in Figure 6c where Node 5 acts as a source to all other receptor nodes). The network diagram corresponding to this single row is shown in Figure 6d. Sediment from Node 5 travels to 30.6% of all nodes, principally to nearby nodes on the ebb-tidal delta and in the main channels. When this procedure is repeated for each of the source nodes, we obtain a complete weighted, directed adjacency matrix (Figure 6e). For context, Node 5 is highlighted in a red box. The central diagonal is empty because with the current model set up, it is not possible to differentiate between sediment from a given source that remains in the bed there, and sediment from that source which is mobilized but recirculates or returns. The complete adjacency matrix can also be represented as a network diagram (e.g., Figure 6f), which provides a useful and intuitive means of visualizing connectivity.

### 3.3 Analyzing Connectivity

#### *3.3.1 Network Analysis*

As hypothesized, the network's strongest connections are in the tidal channels and ebb-tidal delta, where hydrodynamic energy is greater. It is important to note again here that waves are not included in this model, only tidal forcing. The strongest connections and hence dominant sediment transport pathways lie along the main inlet channel and across the ebb-tidal delta. This is because the main inlet channel serves as the central drainage point for the basin and is a convergence zone for flows in and out of the basin. Furthermore, the ebb-tidal delta features strong, convoluted currents and abrupt changes in bathymetry, so the sediment fluxes there are large. Conversely, the connections at the rear of the basin are relatively weaker because of the decreased tidal energy to mobilize sediment there. There are also relatively few direct connections between the rear of the basin and the regions offshore/along the coast, since sediment must have both the time and energy to make the longer journey.

**Density**

The entire network (including all sediment size fractions) has a link density $D$ of 30.6% (Figure 6). When we consider only $100\mu m$ sand, the network density $D$ is 30.2% (Figure 7a), whereas the network density for $400\mu m$ sand is only 12.2% (Figure 7b and Table 1). The dominant pathways for $400\mu m$ sand are confined to the main channel (Figure 7d), whereas $100\mu m$ sand also has strong connections within the inner basin and outer delta (Figure 7c). These findings confirm our earlier hypotheses about expected differences in connectivity as a function of grain size.

However, the differences in connectivity for each grain size class cannot be explained solely by hydrodynamic forcing: connectivity can be supply-limited. The connection between a given source and receptor is also dependent on the availability of that sediment class at the source location. For instance, lack of connection for 400 $\mu$m sand from the rear of the basin (e.g., Node 25) to the outer coast (e.g., Node 14) can be attributed to the relative absence of that sediment class there (Figure 5b).

When link density is considered as a function of time, we see that connectivity increases rapidly during the initial timesteps of the simulation, apparently due to the connection of sediment from sources to their immediate neighbours (Figure 7e). In subse-

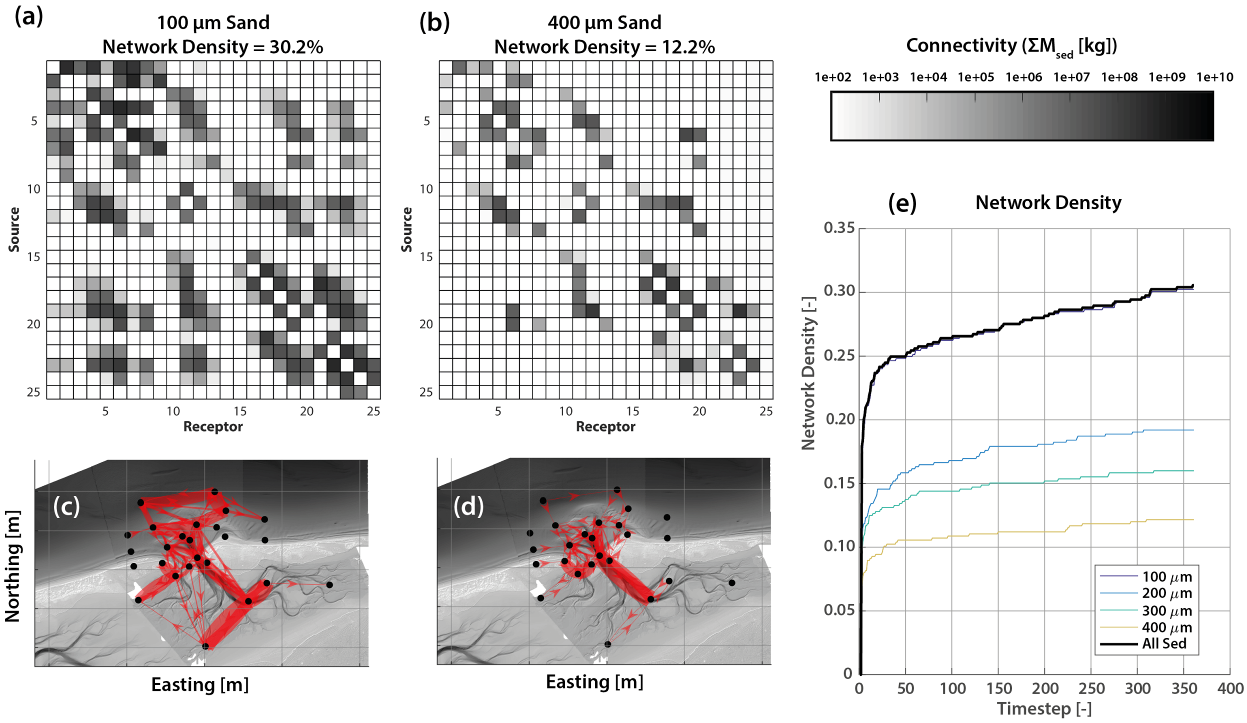


**Figure 7.** Connectivity matrices and network for 100$\mu m$ (a,c) and 400$\mu m$ sand (b,d). To illustrate the dominant patterns, only the top 10% strongest connections are displayed in (c) and (d). (e) Time series of network density $D$, the fraction of actual connections over potential connections.

**Table 1.** Comparison of different connectivity metrics. Network link density, $D$, represents the fraction of actual connections out of all potential connections in the network. Symmetry ($s$) indicates the proportion of reciprocal connections between nodes, where 1 indicates perfect symmetry and 0 indicates complete asymmetry. Modularity ($Q$) lies between -1 and 1, where positive numbers indicate a non-random tendency to form non-overlapping groups [*Rubinov and Sporns*, 2010].

| Scenario | $D[-]$ | $s[-]$ | $Q[-]$ |
|---|---|---|---|
| All Sediment | 0.306 | 0.292 | 0.455 |
| $d_{50} = 100\mu m$ | 0.302 | 0.276 | 0.465 |
| $d_{50} = 200\mu m$ | 0.192 | 0.349 | 0.432 |
| $d_{50} = 300\mu m$ | 0.160 | 0.401 | 0.406 |
| $d_{50} = 400\mu m$ | 0.122 | 0.337 | 0.408 |

quent timesteps, the rate of increase in link density slows considerably, suggestive of a more gradual diffusion after the main connections in the network have been made: sediment must travel greater distances to make new connections.

**Asymmetry**

All of the networks are asymmetric ($s < 1$), which suggests that the system is characterized by non-zero net transports, and hence morphodynamic change (Table 1). However, the networks are not completely asymmetric ($s \approx 0$), likely due in part to the bidirectional nature of tidal transport. There is also no observable trend in asymmetry with respect to grain size.

Asymmetry in a connectivity matrix implies that sediment exchange between two nodes is unequal: a net transport in one direction. In Figure 8a-b, this can be examined by comparing the $634 \times 10^3 m^3$ of sediment leaving the tidal basin (export) with $902 \times 10^3 m^3$ of sediment arriving in the basin from elsewhere (import). In this case, we see a net import of $268 \times 10^3 m^3$ of sediment in 6 months, which is qualitatively consistent with historical trends for Ameland Basin [*Elias et al.*, 2012]. An exact quantitative comparison with measured sediment import volumes is not meaningful here since the present model neglects waves and wind-driven currents, which are important processes at the study site.

**Modularity**

Modularity is positive, which indicates the emergence of functional sediment-sharing groups at non-random levels (Table 1). There is relatively little variation in modularity for different size fractions, which suggests that the modularity in this case is more strongly controlled by the physical structure of the network and hydrodynamic distribution of energy than it is by grain size.

Five distinct modules or sediment-sharing groups are formed: the basin (yellow), offshore/downdrift coast (teal), ebb-tidal delta and main channels (blue), updrift barrier island (light brown), and far downdrift coast (green) (Figure 8c-d). Although transport does occur between each of these communities, the majority occurs inside of them. For example, Cell 23 is well-connected with many locations in the model domain, but modularity quantitatively shows that it is most closely linked with the basin. This grouping could also be useful for defining geomorphic cells as input for larger-scale connectiv-

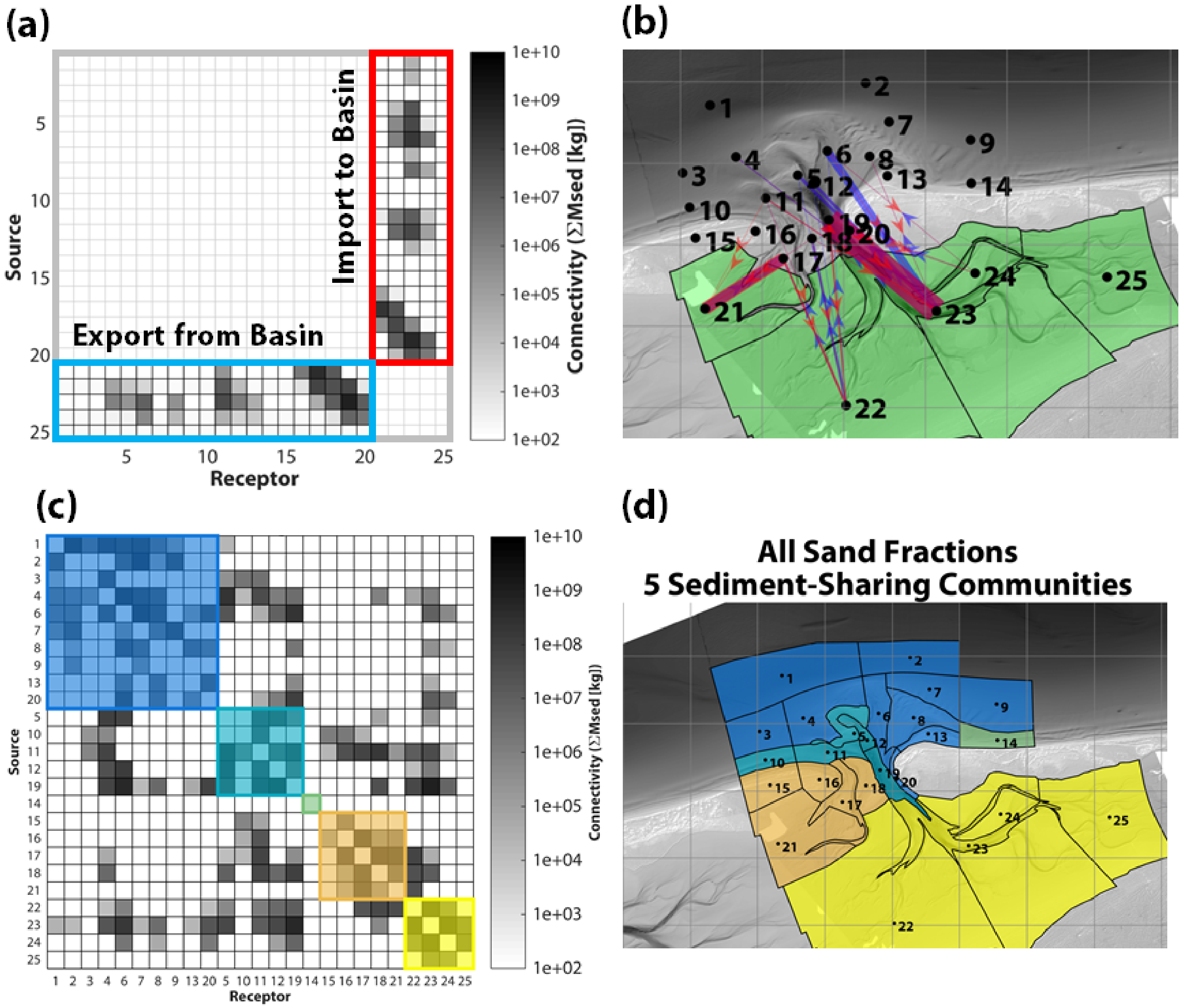


**Figure 8.** Example of different asymmetric connectivity between groups of nodes and modularity. (a) Adjacency matrix filtered to show only connections to (red, “import”) or from (blue, “export”) the inner basin (all grain size classes). Comparing the relative import and export reveals a net import of sediment, in line with historical trends for the site [*Elias et al.*, 2012]. (b) Network diagram illustrating the filtered adjacency matrix from (a). Cells in the basin are indicated in green. (c) Adjacency matrix sorted into functional sediment-sharing groups using the Louvain modularity algorithm, which maximizes within-group connections and minimizes inter-group connections [*Rubinov and Sporns*, 2010]. Each coloured patch in (c) and (d) indicates one of the five sediment-sharing modules identified for the network (all grain size classes).

ity studies (as per *Rossi et al.* [2014]), or in the development of aggregated models (e.g., ASMITA [*Stive et al.*, 1998]).

#### *3.3.2 Analysis of Individual Nodes & Links*

In addition to statistics which characterize the entire network, it is also possible to assess the role of individual nodes.

**Connectivity between Specific Nodes**

Individual nodes can also be queried to answer specific questions. For instance, net sediment import into or export from a tidal basin is a vital quantity for estimating coastal sediment budgets, and can be determined by examining asymmetric connections between nodes lying inside and outside the basin. For this particular simplified model, we see a net import of sediment into the basin (Figure 8a-b). When we examine connections between the updrift and downdrift islands, we find that the shortest pathway (calculated in terms of fluxes, not geometric distance) depends on the offshore distance of the source (Figure 9). Sediment beginning its journey in the nearshore or outer bar region will travel via the inlet (blue and yellow lines), whereas sediment originating further offshore will travel via the outer delta.

This suggests that the bypassing routes of interest in Figure 1 depend largely on cross-shore position. Bear in mind that this model uses a schematized tidal signal and neglects key processes known to be important for bypassing, such as waves and wind-induced currents. As such, these pathways should be re-evaluated using a more comprehensive model.

**Degree, Strength, & Betweenness Centrality**

When nodes in our network are considered individually, we see that the nodes with highest degree and strength are generally those in the main channels and on the ebb-tidal delta (Figure 10a,b), which follows from the earlier observations on network density (Figure 7). Nodes in the main channel also have the highest betweenness centrality, which confirms and quantifies our hypothesis about the role of the channel as a transport bottleneck (Figure 10c).

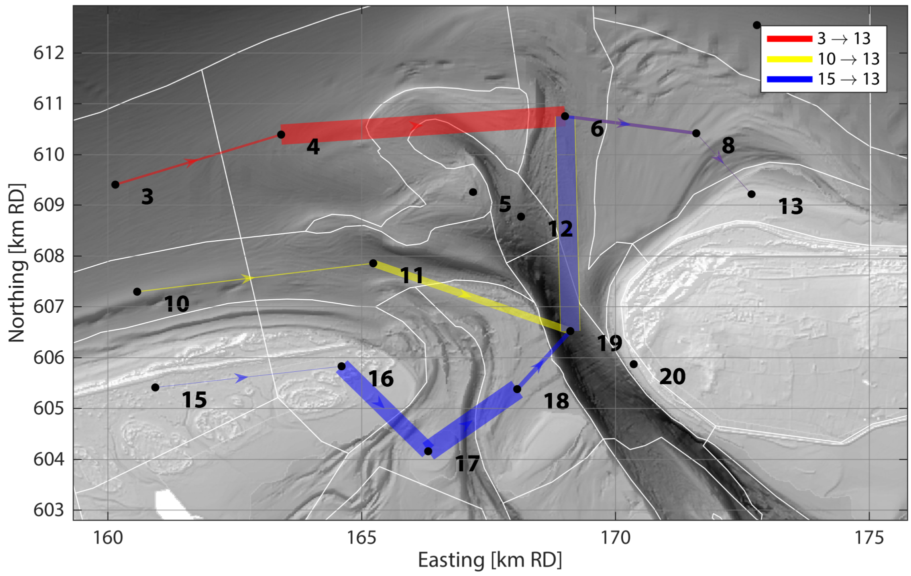


**Figure 9.** Shortest inlet bypassing pathway for different initial locations on the updrift side of the inlet. Path "distance" is inversely proportional to sediment flux, such that stronger fluxes (indicated here by thicker lines) are effectively "shorter" topological distances. Sources closer to the updrift coastline (10, 15) are connected to the downdrift coast via the inlet, whereas the offshore source (3) is connected via the outer delta. Note that the underlying model presented here does not account for wave-driven bypassing

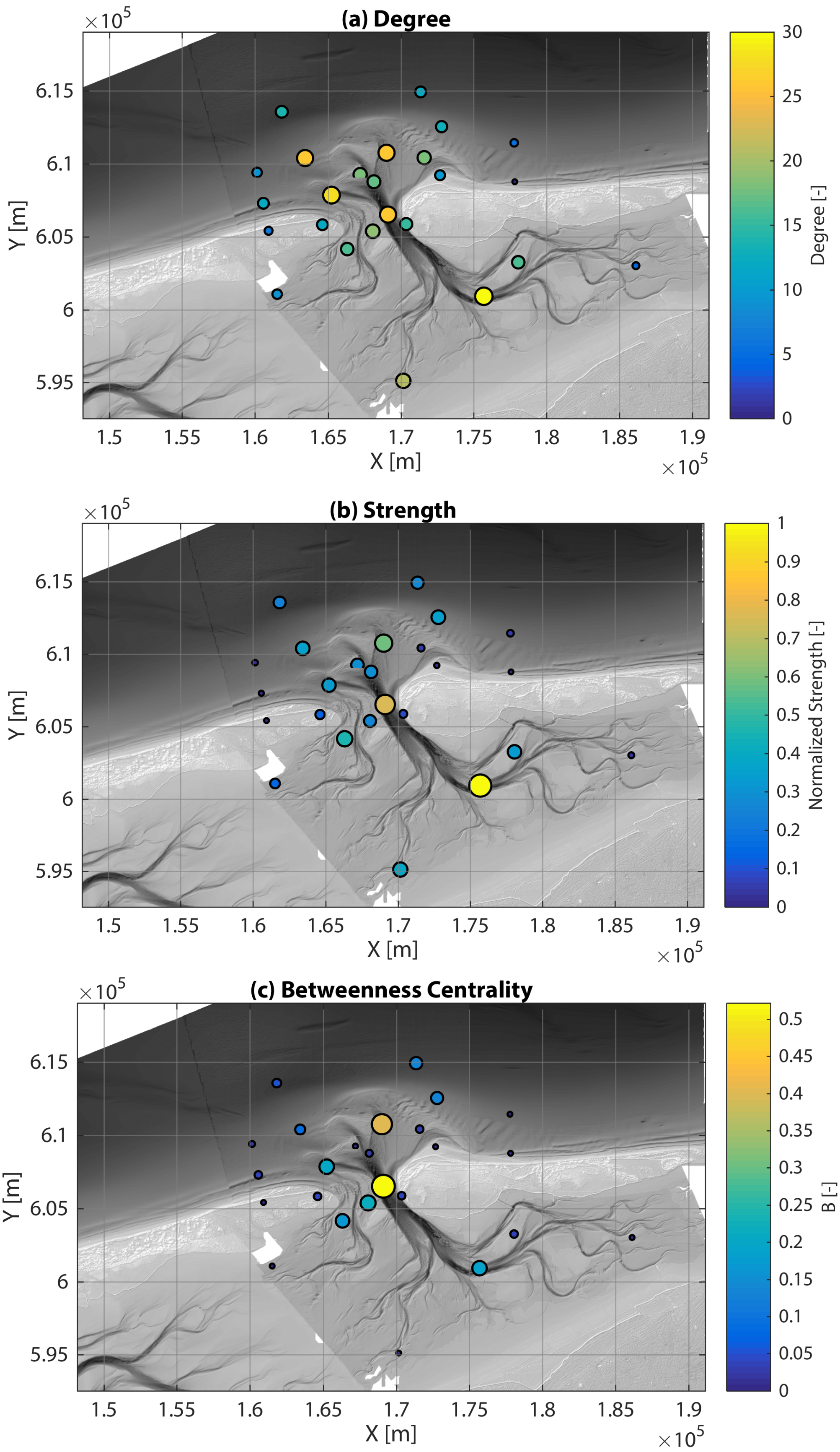


694 **Figure 10.** Connectivity metrics for individual nodes. (a) Total degree $D$ (in-degree plus
695 out-degree). (b) Total strength $S$ (in-strength plus out-strength) normalized by the node of
696 maximum strength. (c) Betweenness centrality, $B$, normalized by the total number of pathways
697 between nodes (n=625).

### 3.4 Summary

This case study for Ameland Inlet was intended to show a proof of concept for how sediment connectivity could be applied to a real coastal example. The most challenging part of the approach was to configure and run the model in such a way that sediment pathways could be defined. However, once the data was compiled into a network, sediment transport patterns could be easily quantified using metrics like asymmetry, modularity, and betweenness. The availability of free, open-source analysis tools makes connectivity analysis a highly accessible approach, which yields useful insights into sediment transport at both local and system levels.

## 4 Discussion

The sediment connectivity framework brings many new and useful opportunities for analyzing coastal sediment transport pathways. Connectivity provides tools to quantify the dominant transport pathways for sediment originating from or leading to a particular location. Already well-established in other disciplines, these techniques allow us to identify salient features of transport pathways that may be relevant for both fundamental understanding of a given coastal system, and for answering applied engineering questions. We demonstrated this by applying the approach to Ameland Inlet and addressing the example research questions posed in Figure 1. The analysis presented here is intended to demonstrate the usefulness of sediment connectivity for coastal applications and encourage its use in future studies.

Connectivity brings value to existing numerical coastal models by adding techniques in graph theory and network analysis to the "toolkit" available for interpreting sediment pathways from those models. Once sediment transport is represented in an adjacency matrix, then computing statistical metrics of connectivity using existing tools (e.g., *Csárdi and Nepusz* [2006]; *Rubinov and Sporns* [2010]; *Franz et al.* [2016]) is straightforward. These techniques can quantify spatial and temporal variations in sediment transport beyond just existing metrics like cumulative erosion and sedimentation patterns or mean transport fields. With connectivity, we have mathematical techniques for describing not just where sediment is going, but *which* sediment is going where. However it is more useful than Lagrangian modelling alone, because it tells us not only the history of sediment from a particular source, it tells us something about the interconnected coastal system as a whole.

There are many possible metrics for evaluating connectivity, although we believe that the ones presented in this study are the most useful for studying sediment pathways in coastal systems. They provide concrete means of quantifying intuitive and useful but abstract concepts such as centrality or modularity. The metrics shown here are also useful for addressing practical engineering and management problems. For instance, the strength of nodes can be used to optimize dredging and nourishment strategies.

It is widely acknowledged that the question of scaling (both temporal and spatial) is still a huge challenge for quantifying connectivity [*Wohl et al.*, 2019; *Bracken et al.*, 2015; *Keesstra et al.*, 2018]. *Keesstra et al.* [2018] maintain that there is still "no satisfactory solution to the problem of scaling in water and sediment connectivity". Furthermore, the issue of separating structural and functional connectivity is still unresolved in most disciplines using connectivity [*Turnbull et al.*, 2018]. This problem is related to the time scaling issues described above, since eventually sediment fluxes modify morphology. Tied to the separation of form and function is the definition of the fundamental unit of connectivity. Geomorphic cells defined based on structural criteria like bathymetry will shift from their original boundaries after sufficient fluxes of sediment modify the seabed. Although these open questions present challenges to coastal researchers looking to apply connectivity, they also present opportunities: connectivity could be a useful approach for exploring sediment transport pathways at varying spatial and temporal scales.

Recent advances in remote sensing, in situ measurements, and numerical modelling have created a wealth of data for coastal researchers [*Donchyts et al.*, 2016; *Ford and Dickson*, 2018; *Luijendijk et al.*, 2018; *Vos et al.*, 2019]. In this era of "big data", we need a standardized framework to integrate and compare the coastal sediment pathways derived from models and field data. Since it may be difficult to validate connectivity computed from a single model, this approach would allow multiple lines of evidence or modelled ensemble predictions to be integrated in a common framework (similarly to *Barnard et al.* [2013b]), increasing confidence in the predictions made. Future research should also assess the applicability of alternative modelling techniques (e.g., Lagrangian particle tracking [*Soulsby et al.*, 2011; *MacDonald and Davies*, 2007] or directly computing connectivity from Eulerian transport fields) for connectivity analysis.

Connectivity also distils complex systems into their basic essence in a visually-effective manner (e.g., subway maps [*Derrible and Kennedy*, 2009]). Furthermore, online visualization tools (e.g., Cytoscape [*Franz et al.*, 2016]) make it possible to develop interactive ways of visualizing connectivity, bringing tangible form to the often abstract concepts of sediment transport. This also makes connectivity an attractive platform for communicating with stakeholders and the public.

*Phillips et al.* [2015] note that connectivity analysis using graph theory "should certainly be included on the standard menu of relevant methods" for geoscientists. Wider adoption of the connectivity concept in coastal geoscience will yield further improvements to the method's usefulness, and hopefully inspire new solutions to existing problems.

## 5 Conclusions

Sediment connectivity quantifies how different locations are connected by sediment transport pathways. The concept of connectivity is well-established in other disciplines, and here we use the example of Ameland Inlet to demonstrate its utility in coastal sediment transport settings. Connectivity provides a framework for identifying, analyzing, and interpreting sediment pathways in complex coastal systems.

By dividing a system into geomorphic cells and quantifying the transports between them, we can populate an adjacency matrix and network graph. In that form, existing techniques in graph theory and network analysis offer novel ways of quantifying coastal sediment transport, revealing patterns that may not be obvious with existing techniques. In the case of Ameland Inlet, density, asymmetry, and modularity are used to quantify sediment transport patterns at a system level. Other metrics like degree, strength, centrality, and shortest-path analysis are used to identify critical paths or locations within the system. These parameters give insight into natural coastal dynamics and are also useful for optimizing engineering interventions (e.g., sand nourishments).

The case study of Ameland Inlet shows the potential for connectivity to quantify sediment transport pathways in coastal systems. We believe that this approach has the potential to become a standard tool, and that it will be valuable for addressing some of the urgent problems facing our coasts in the 21st century.

**Acknowledgments**

This work is part of the research programme Collaboration Program Water with project number 14489 (SEAWAD), which is (partly) financed by NWO Domain Applied and Engineering Sciences. Special thanks to the Dutch Ministry of Infrastructure and Water Management (Rijkswaterstaat and Rijksrederij) for their ongoing support as part of the Kustgenese2.0 project. We are grateful to Klaas Lenstra, [USGS Internal Reviewer], and [two anonymous reviewers] for their constructive feedback. Data archiving for this study is currently underway. Model input files used in this study have been included as supplementary material for the review process. The data under consideration will be stored openly in compliance with FAIR Data standards on the 4TU data repository (https://data.4tu.nl/) at DOI 10.4121/uuid:9879475e-03a8-4f54-8b78-83e6dae287f8, upon acceptance of the manuscript. The connectivity analysis in this study was carried out using the open-source Brain Connectivity Toolbox (https://sites.google.com/site/bctnet/).

## References

Bak, J. (2017), Nourishment strategies for Ameland Inlet, Master's thesis, Delft University of Technology.

Barnard, P. L., L. H. Erikson, E. P. L. Elias, and P. Dartnell (2013a), Sediment transport patterns in the San Francisco Bay Coastal System from cross-validation of bedform asymmetry and modeled residual flux, *Marine Geology*, *345*(November), 72–95, doi:10.1016/j.margeo.2012.10.011.

Barnard, P. L., A. C. Foxgrover, E. P. L. Elias, L. H. Erikson, J. R. Hein, M. McGann, K. Mizell, R. J. Rosenbauer, P. W. Swarzenski, R. K. Takesue, F. L. Wong, and D. L. Woodrow (2013b), Integration of bed characteristics, geochemical tracers, current measurements, and numerical modeling for assessing the provenance of beach sand in the San Francisco Bay Coastal System, *Marine Geology*, *345*, 181–206, doi:10.1016/j.margeo.2013.08.007.

Barry, S. J., P. J. Cowell, and C. D. Woodroffe (2007), A morphodynamic model of reef-island development on atolls, *Sedimentary Geology*, *197*(1-2), 47–63, doi:10.1016/j.sedgeo.2006.08.006.

Bartholdy, J., A. Bartholomä, and B. W. Flemming (2002), Grain Size Control Of Large Compound Flow Transverse Bedforms In A Tidal Inlet Of The Danish Wadden Sea, *Marine Geology*, *188*, 391–413.

Bassett, D. S., D. L. Greenfield, A. Meyer-Lindenberg, D. R. Weinberger, S. W. Moore, and E. T. Bullmore (2010), Efficient physical embedding of topologically complex information processing networks in brains and computer circuits, *PLoS Computational Biology*, *6*(4), doi:10.1371/journal.pcbi.1000748.

Beck, T. M., and P. Wang (2019), Morphodynamics of barrier-inlet systems in the context of regional sediment management , with case studies from west-central Florida , USA, *Ocean and Coastal Management*, *177*(April), 31–51, doi: 10.1016/j.ocecoaman.2019.04.022.

Black, K. S., S. Athey, P. Wilson, and D. Evans (2007), The use of particle tracking in sediment transport studies: a review, *Geological Society, London, Special Publications*, *274*(1), 73–91, doi:10.1144/GSL.SP.2007.274.01.09.

Bosnic, I., J. Cascalho, R. Taborda, T. Drago, J. Hermínio, M. Rosa, J. Dias, and E. Garel (2017), Nearshore sediment transport: coupling sand tracer dynamics with oceanographic forcing, *Marine Geology*, *385*, 293–303, doi: 10.1016/j.margeo.2017.02.004.

Bracken, L. J., L. Turnbull, J. Wainwright, and P. Bogaart (2015), Sediment connectivity: A framework for understanding sediment transfer at multiple scales, *Earth Surface Processes and Landforms*, *40*(2), 177–188, doi:10.1002/esp.3635.

Brakenhoff, L., M. Kleinhans, G. Ruessink, and M. Vegt (2019), Spatiotemporal characteristics of smallscale wavecurrent ripples on the Ameland ebbtidal delta, *Earth Surface Processes and Landforms*, doi:10.1002/esp.4802.

Burgess, S. C., K. J. Nickols, C. D. Griesemer, L. a. K. Barnett, A. G. Dedrick, E. V. Satterthwaite, L. Yamane, S. G. Morgan, J. W. White, and L. W. Botsford (2013), Beyond connectivity: how empirical methods can quantify population persistence to improve marine protected area design, *Ecological Applications*, p. 130819190545008, doi:10.1890/13-0710.1.

Calabrese, J. M., and W. F. Fagan (2004), A comparison-shopper's guide to connectivity metrics, *Frontiers in Ecology and the Environment*, *2*(10), 529–536, doi:10.1890/1540-9295(2004)002[0529:ACGTCM]2.0.CO;2.

Cantwell, M. D., and R. T. T. Forman (1993), Landscape graphs: Ecological modeling with graph theory to detect configurations common to diverse landscapes, *Landscape Ecology*, *8*(4), 239–255.

Condie, S. A., M. Herzfeld, K. Hock, J. R. Andrewartha, R. Gorton, R. Brinkman, and M. Schultz (2018), System level indicators of changing marine connectivity, *Ecological Indicators*, *91*(November 2017), 531–541, doi: 10.1016/j.ecolind.2018.04.036.

Cossart, E., V. Viel, C. Lissak, R. Reulier, M. Fressard, and D. Delahaye (2018), How might sediment connectivity change in space and time?, *Land Degradation and Development*, *29*(8), 2595–2613, doi:10.1002/ldr.3022.

Cowen, R. K., and S. Sponaugle (2009), Larval Dispersal and Marine Population Connectivity, *Annu. Rev. Mar. Sci*, *1*, 443–466, doi: 10.1146/annurev.marine.010908.163757.

Csárdi, G., and T. Nepusz (2006), The igraph software package for complex network research, *InterJournal Complex Systems*, *1695*, 1–9, doi: 10.3724/SP.J.1087.2009.02191.

Davis, R. A. J., and P. L. Barnard (2000), How anthropogenic factors in the back-barrier area influence tidal inlet stability: examples from the Gulf Coast of Florida, USA, *Geological Society London Special Publications*, *175*(1), 293, doi: 10.1144/GSL.SP.2000.175.01.21.

de Fockert, A. (2008), Impact of Relative Sea Level Rise on the Amelander Inlet Morphology, Master, TU Delft.

De Wit, F., M. Tissier, and A. Reniers (2019), Characterizing wave shape evolution on an ebb-tidal shoal, *Journal of Marine Science and Engineering*, pp. 1–20, doi:10.3390/jmse7100367.

Defne, Z., N. K. Ganju, and A. Aretxabaleta (2016), Estimating time-dependent connectivity in marine systems, *Geophysical Research Letters*, *43*(3), 1193–1201, doi:10.1002/2015GL066888.

Derrible, S., and C. Kennedy (2009), Network Analysis of World Subway Systems Using Updated Graph Theory, *Transportation Research Record: Journal of the Transportation Research Board*, *2112*, 17–25, doi:10.3141/2112-03.

Donchyts, G., F. Baart, H. Winsemius, N. Gorelick, J. Kwadijk, and N. Van De Giesen (2016), Earth's surface water change over the past 30 years, *Nature Climate Change*, *6*(9), 810–813, doi:10.1038/nclimate3111.

Duc, D. M., D. X. Thanh, D. T. Quynh, and P. McLaren (2016), Analysis of sediment distribution and transport for mitigation of sand deposition hazard in

Tam Quan estuary, Vietnam, *Environmental Earth Sciences*, *75*(9), 741, doi: 10.1007/s12665-016-5560-2.

Duong, T. M., R. Ranasinghe, D. J. R. Walstra, and D. Roelvink (2016), Assessing climate change impacts on the stability of small tidal inlet systems: Why and how?, *Earth-Science Reviews*, *154*, 369–380, doi:10.1016/j.earscirev.2015.12.001.

Duran-Matute, M., T. Gerkema, G. J. De Boer, J. J. Nauw, and U. Grawe (2014), Residual circulation and freshwater transport in the Dutch Wadden Sea: A numerical modelling study, *Ocean Science*, *10*(4), 611–632, doi:10.5194/os-10-611-2014.

Eelkema, M., Z. B. Wang, A. Hibma, and M. J. F. Stive (2013), Morphological Effects of the Eastern Scheldt Storm Surge Barrier on the Ebb-Tidal Delta, *Coastal Engineering Journal*, *55*(03), 1350,010, doi:10.1142/S0578563413500101.

Elias, E. P. L., and J. E. Hansen (2013), Understanding processes controlling sediment transports at the mouth of a highly energetic inlet system (San Francisco Bay, CA), *Marine Geology*, *345*(November 2013), 207–220, doi: 10.1016/j.margeo.2012.07.003.

Elias, E. P. L., and A. J. F. Van Der Spek (2006), Long-term morphodynamic evolution of Texel Inlet and its ebb-tidal delta (The Netherlands), *Marine Geology*, *225*(1-4), 5–21, doi:10.1016/j.margeo.2005.09.008.

Elias, E. P. L., J. Cleveringa, M. C. Buijsman, J. Roelvink, M. J. F. M. Stive, D. Roelvink, and M. J. F. M. Stive (2006), Field and model data analysis of sand transport patterns in Texel Tidal inlet (the Netherlands), *Coastal Engineering*, *53*(5-6), 505–529, doi:10.1016/j.coastaleng.2005.11.006.

Elias, E. P. L., G. Gelfenbaum, M. Van Ormondt, and H. R. Moritz (2011), Predicting sediment transport patterns at the mouth of the Columbia River, *Proc. Coastal Sediments. 2011*, pp. 588–601.

Elias, E. P. L., A. J. F. van der Spek, Z. B. Wang, and J. De Ronde (2012), Morphodynamic development and sediment budget of the Dutch Wadden Sea over the last century, *Geologie en Mijnbouw/Netherlands Journal of Geosciences*, *91*(3), 293–310, doi:10.1017/S0016774600000457.

Elias, E. P. L., R. Teske, A. J. F. van der Spek, and M. Lazar (2015), Modelling Tidal-Inlet Morphodynamics on Medium Time Scales, in *Coastal Sediments 2015*, pp. 1–14, San Diego, CA.

Elias, E. P. L., A. J. F. Van Der Spek, S. G. Pearson, and J. Cleveringa (2019), Understanding sediment bypassing processes through analysis of high- frequency observations of Ameland Inlet , the Netherlands, *Marine Geology*, *415*(May), 105,956, doi:10.1016/j.margeo.2019.06.001.

Erikson, L. H., S. a. Wright, E. P. L. Elias, D. M. Hanes, D. H. Schoellhamer, and J. L. Largier (2013), The use of modeling and suspended sediment concentration measurements for quantifying net suspended sediment transport through a large tidally dominated inlet, *Marine Geology*, *345*, 96–112, doi: 10.1016/j.margeo.2013.06.001.

Esposito, U., M. Giugliano, M. Van Rossum, and E. Vasilaki (2014), Measuring symmetry, asymmetry and randomness in neural network connectivity, *PLoS ONE*, *9*(7), doi:10.1371/journal.pone.0100805.

FitzGerald, D. M. (1982), Sediment Bypassing At Mixed Energy Tidal Inlets., *Proceedings of the Coastal Engineering Conference*, *2*, 1094–1118, doi: 10.9753/icce.v18.68.

FitzGerald, D. M. (1984), Interactions between the ebb-tidal delta and landward shoreline; Price Inlet, South Carolina, *Journal of Sedimentary Research*, *54*(4), 1303–1318, doi:10.1306/212F85C6-2B24-11D7-8648000102C1865D.

Fontolan, G., S. Pillon, F. Delli Quadri, and A. Bezzi (2007), Sediment storage at tidal inlets in northern Adriatic lagoons: Ebb-tidal delta morphodynamics, conservation and sand use strategies, *Estuarine, Coastal and Shelf Science*, *75*(1-2), 261–277, doi:10.1016/j.ecss.2007.02.029.

Ford, M. R., and M. E. Dickson (2018), Detecting ebb-tidal delta migration using Landsat imagery, *Marine Geology*, *405*(December 2017), 38–46, doi: 10.1016/j.margeo.2018.08.002.

Franz, M., C. T. Lopes, G. Huck, Y. Dong, O. Sumer, and G. D. Bader (2016), Cytoscape.js: A graph theory library for visualisation and analysis, *Bioinformatics*, *32*(2), 309–311, doi:10.1093/bioinformatics/btv557.

Friedrichs, C. T. (2012), *Tidal Flat Morphodynamics: A Synthesis*, vol. 3, 137–170 pp., Elsevier Inc., doi:10.1016/B978-0-12-374711-2.00307-7.

Fryirs, K. (2013), (Dis)Connectivity in catchment sediment cascades: A fresh look at the sediment delivery problem, *Earth Surface Processes and Landforms*, *38*(1), 30–46, doi:10.1002/esp.3242.

Gao, S., and M. Collins (1991), Discussion: A Critique of the "McLaren Method" for Defining Sediment Transport Paths, *Journal of Sedimentary Petrology*, *61*(1), 143–146.

Gartner, J. W., R. T. Cheng, P. F. Wang, and K. Richter (2001), Laboratory and field evaluations of the LISST-100 instrument for suspended particle size determinations, *Marine Geology*, *175*(1-4), 199–219, doi:10.1016/S0025-3227(01)00137-2.

Gaudiano, D. J., and T. W. Kana (2001), Shoal Bypassing in Mixed Energy Inlets: Geomorphic Variables and Empirical Predictions for Nine South Carolina Inlets, *Journal of Coastal Research*, *17*(2), 280–291.

Gelfenbaum, G., E. P. L. Elias, and A. W. Stevens (2017), Investigation of Input Reduction Techniques for Morphodynamic Modelling of Complex Inlets with Baroclinic Forcing, in *Coastal Dynamics 2017*, 260, pp. 1142–1154, Helsingor, Denmark.

Gillanders, B. M., T. S. Elsdon, and M. Roughan (2012), *Connectivity of Estuaries*, vol. 7, 119–142 pp., Elsevier Inc., doi:10.1016/B978-0-12-374711-2.00709-9.

Grober-Dunsmore, S. J. Pittman, C. Caldow, M. S. Kendall, and T. K. Frazer (2009), *Ecological Connectivity among Tropical Coastal Ecosystems*, 1–615 pp., Springer Netherlands, Dordrecht, doi:10.1007/978-90-481-2406-0.

Hanley, M. E., S. P. G. Hoggart, D. J. Simmonds, A. Bichot, M. A. Colangelo, F. Bozzeda, H. Heurtefeux, B. Ondiviela, R. Ostrowski, M. Recio, R. Trude, E. Zawadzka-kahlau, and R. C. Thompson (2014), Shifting sands ? Coastal protection by sand banks , beaches and dunes, *Coastal Engineering*, *87*, 136–146, doi:10.1016/j.coastaleng.2013.10.020.

Hansen, J. E., E. P. L. Elias, and P. L. Barnard (2013), Changes in surfzone morphodynamics driven by multi-decadal contraction of a large ebb-tidal delta, *Marine Geology*, *345*, 221–234, doi:10.1016/j.margeo.2013.07.005.

Hanson, H., A. Brampton, M. Capobianco, H. H. Dette, L. Hamm, C. Laustrup, A. Lachuga, and R. Spanhoff (2002), Beach nourishment projects, practices and objectives  a European overview, *Coastal Engineering*, *47*(0378), 81–111.

Hayes, M. O. (1980), General morphology and sediment patterns in tidal inlets, *Sedimentary Geology*, *26*(1-3), 139–156, doi:10.1016/0037-0738(80)90009-3.

Heckmann, T., and W. Schwanghart (2013), Geomorphic coupling and sediment connectivity in an alpine catchment - Exploring sediment cascades using graph theory, *Geomorphology*, *182*, 89–103, doi:10.1016/j.geomorph.2012.10.033.

Heckmann, T., W. Schwanghart, and J. D. Phillips (2014), Graph theory-Recent developments of its application in geomorphology, *Geomorphology*, *243*, 130–146, doi:10.1016/j.geomorph.2014.12.024.

Heckmann, T., M. Cavalli, O. Cerdan, S. Foerster, M. Javaux, E. Lode, A. Smetanova, D. Vericat, and F. Brardinoni (2018), Indices of sediment connectivity: opportunities, challenges and limitations, *Earth-Science Reviews*, p. #pagerange#, doi:10.1016/J.EARSCIREV.2018.08.004.

Hein, J. R., K. Mizell, and P. L. Barnard (2013), Sand sources and transport pathways for the San Francisco Bay coastal system, based on X-ray diffraction mineralogy, *Marine Geology*, *345*, 154–169, doi:10.1016/j.margeo.2013.04.003.

Herrling, G., and C. Winter (2014), Morphological and sedimentological response of a mixed-energy barrier island tidal inlet to storm and fair-weather conditions, *Earth Surface Dynamics*, *2*(1), 363–382, doi:10.5194/esurf-2-363-2014.

Herrling, G., and C. Winter (2018), Tidal inlet sediment bypassing at mixed-energy barrier islands, *Coastal Engineering*, *140*(October 2017), 342–354, doi:10.1016/j.coastaleng.2018.08.008.

Hiatt, M., W. Sonke, E. A. Addink, W. M. V. Dijk, and M. V. Kreveld (2019), Geometry and Topology of Estuary and Braided River Channel Networks Automatically Extracted From Topographic Data, pp. 1–19, doi:10.1029/2019JF005206.

Hicks, M. D., T. M. Hume, A. Swales, and M. O. Green (1999), Magnitudes, spacial extent, time scales and causes of shoreline change adjacent to an ebb tidal delta, Katikati Inlet, New Zealand, *Journal of Coastal Research*, *15*(1), 220–240, doi:10.1590/S0100-67622003000600004.

Hock, K., N. H. Wolff, J. C. Ortiz, S. A. Condie, K. R. Anthony, P. G. Blackwell, and P. J. Mumby (2017), Connectivity and systemic resilience of the Great Barrier Reef, *PLoS Biology*, *15*(11), 1–23, doi:10.1371/journal.pbio.2003355.

Honey, C. J., R. Kötter, M. Breakspear, and O. Sporns (2007), Network structure of cerebral cortex shapes functional connectivity on multiple time scales., *Proceedings of the National Academy of Sciences*, *104*(24), 10,240–10,245, doi:10.1073/pnas.0701519104.

Huisman, B. J., B. G. Ruessink, M. A. de Schipper, A. P. Luijendijk, and M. J. Stive (2018), Modelling of bed sediment composition changes at the lower shoreface of the Sand Motor, *Coastal Engineering*, *132*(November 2017), 33–49, doi:10.1016/j.coastaleng.2017.11.007.

Jaffe, B. E., J. H. List, and A. H. Sallenger (1997), Massive sediment bypassing on the lower shoreface offshore of a wide tidal inlet - Cat Island Pass, Louisiana, *Marine Geology*, *136*(3-4), 131–149, doi:10.1016/S0025-3227(96)00050-3.

Jeuken, M. C. J. L., and Z. B. Wang (2010), Impact of dredging and dumping on the stability of ebb-flood channel systems, *Coastal Engineering*, *57*(6), 553–566, doi:10.1016/j.coastaleng.2009.12.004.

Kana, T. W., E. J. Hayter, and P. a. Work (1999), Mesoscale Sediment Transport at Southeastern U.S. Tidal Inlets: Conceptual Model Applicable to Mixed Energy Settings, *Journal of Coastal Research*, *15*(2), pp. 303—-313.

Keesstra, S., J. Pedro, P. Saco, T. Parsons, R. Poeppl, R. Masselink, and A. Cerdà (2018), The way forward: Can connectivity be useful to design better measuring and modelling schemes for water and sediment dynamics?, *Science of The Total Environment*, *644*, 1557–1572, doi:10.1016/J.SCITOTENV.2018.06.342.

Kindlmann, P., and F. Burel (2008), Connectivity measures: A review, *Landscape Ecology*, *23*(8), 879–890, doi:10.1007/s10980-008-9245-4.

Koohafkan, M. C., and S. Gibson (2018), Geomorphic trajectory and landform analysis using graph theory, *Progress in Physical Geography: Earth and Environment*, p. 030913331878314, doi:10.1177/0309133318783143.

Kool, J. T., A. Moilanen, and E. A. Treml (2013), Population connectivity: Recent advances and new perspectives, *Landscape Ecology*, *28*(2), 165–185, doi:10.1007/s10980-012-9819-z.

Krause, J., D. P. Croft, and R. James (2007), Social network theory in the behavioural sciences : potential applications, pp. 15–27, doi:10.1007/s00265-007-0445-8.

Kundu, P. K., and I. M. Cohen (2008), *Fluid Mechanics*, 4th ed., 872 pp., Elsevier, Burlington, MA.

Latteux, B. (1995), Techniques for long-term morphological simulation under tidal action, *Marine Geology*, *126*(1-4), 129–141, doi:10.1016/0025-3227(95)00069-B.

Le Roux, J. P., and E. M. Rojas (2007), Sediment transport patterns determined from grain size parameters: Overview and state of the art, *Sedimentary Geology*, *202*(3), 473–488, doi:10.1016/j.sedgeo.2007.03.014.

Leicht, E. A., and M. E. Newman (2008), Community structure in directed networks, *Physical Review Letters*, *100*(11), 1–4, doi: 10.1103/PhysRevLett.100.118703.

Lenstra, K. J., S. R. Pluis, W. Ridderinkhof, G. Ruessink, and M. van der Vegt (2019), Cyclic channel-shoal dynamics at the Ameland inlet: the impact on waves, tides, and sediment transport, *Ocean Dynamics*, *69*(4), 409–425, doi: 10.1007/s10236-019-01249-3.

Lesser, G. R., D. Roelvink, J. a. T. M. van Kester, and G. S. Stelling (2004), Development and validation of a three-dimensional morphological model, *Coastal Engineering*, *51*(8-9), 883–915, doi:10.1016/j.coastaleng.2004.07.014.

Lodder, Q. J., Z. B. Wang, E. P. Elias, A. J. van der Spek, H. de Looff, and I. H. Townend (2019), Future response of thewadden sea tidal basins to relative sea-level rise-an aggregated modelling approach, *Water (Switzerland)*, *11*(10), doi: 10.3390/w11102198.

Luijendijk, A., G. Hagenaars, R. Ranasinghe, F. Baart, G. Donchyts, and S. Aarninkhof (2018), The State of the World's Beaches, *Scientific Reports*, *8*(1), 6641, doi:10.1038/s41598-018-24630-6.

Luijendijk, A. P., R. Ranasinghe, M. A. de Schipper, B. A. Huisman, C. M. Swinkels, D. J. R. Walstra, and M. J. F. Stive (2017), The initial morphological response of the Sand Engine: A process-based modelling study, *Coastal Engineering*, *119*(August 2015), 1–14, doi:10.1016/j.coastaleng.2016.09.005.

MacDonald, N. J., and M. H. Davies (2007), Particle-Based Sediment Transport Modelling, in *Coastal Engineering 2006*, vol. 3, pp. 3117–3128, World Scientific Publishing Company.

Maslov, S., and K. Sneppen (2002), Specificity and Stability in Topology of Protein Networks, *Science*, *296*(5569), 910–913, doi:10.1126/science.1065103.

Masselink, G., A. Kroon, and R. G. D. Davidson-arnott (2006), Morphodynamics of intertidal bars in wave-dominated coastal settings  A review, *73*, 33–49, doi: 10.1016/j.geomorph.2005.06.007.

McGann, M., L. Erikson, E. Wan, C. Powell, and R. F. Maddocks (2013), Distribution of biologic, anthropogenic, and volcanic constituents as a proxy for sediment transport in the San Francisco Bay Coastal System, *Marine Geology*, *345*, 113–142, doi:10.1016/j.margeo.2013.05.006.

McLachlan, R. L., A. S. Ogston, N. E. Asp, A. T. Fricke, C. A. Nittrouer, and V. J. Gomes (2020), Impacts of tidal-channel connectivity on transport asymmetry and sediment exchange with mangrove forests, *Estuarine, Coastal and Shelf Science*, *233*, 106,524, doi:10.1016/j.ecss.2019.106524.

McLaren, P. (2013), Sediment Trend Analysis (STA ®): Kinematic vs. Dynamic Modeling, *Journal of Coastal Research*, *30*(3), 429–437, doi: 10.2112/JCOASTRES-D-13-00121.1.

McLaren, P., and D. Bowles (1985), The Effects of Sediment Transport on Grain Size Distributions, *Journal of Sedimentary Petrology*, *55*(4), 0457–0470.

McLaren, P., F. Steyaert, and R. Powys (1998), Sediment Transport Studies in the Tidal Basins of the Dutch Waddenzee, *Senckenbergiana Maritima*, *29*(1), 53–61.

Moilanen, A. (2011), On the limitations of graph-theoretic connectivity in spatial ecology and conservation, *Journal of Applied Ecology*, *48*(6), 1543–1547, doi: 10.1111/j.1365-2664.2011.02062.x.

Mulder, J. P. M., S. Hommes, and E. M. Horstman (2011), Ocean & Coastal Management Implementation of coastal erosion management in the Netherlands, *Ocean and Coastal Management*, *54*(12), 888–897, doi:10.1016/j.ocecoaman.2011.06.009.

Newman, M. E. J. (2003), The Structure and Function of Complex Networks, *SIAM*, *45*(2), 167–256.

Nienhuis, J. H., and A. D. Ashton (2016), Mechanics and rates of tidal inlet migration: Modeling and application to natural examples, *Journal of Geophysical Research: Earth Surface*, *121*(11), 2118–2139, doi:10.1002/2016JF004035.

Oertel, G. (1972), Sediment transport of estuary entrance shoals and the formation of swash platforms, *Journal of Sedimentary Research*, *42*(4), 858–863, doi: 10.1306/74D72658-2B21-11D7-8648000102C1865D.

Paris, C. B., J. Helgers, E. van Sebille, and A. Srinivasan (2013), Connectivity Modeling System: A probabilistic modeling tool for the multi-scale tracking of biotic and abiotic variability in the ocean, *Environmental Modelling and Software*, *42*, 47–54, doi:10.1016/j.envsoft.2012.12.006.

Passalacqua, P. (2017), The Delta Connectome: A network-based framework for studying connectivity in river deltas, *Geomorphology*, *277*, 50–62, doi: 10.1016/j.geomorph.2016.04.001.

Phillips, J. D., W. Schwanghart, and T. Heckmann (2015), Graph theory in the geosciences, *Earth-Science Reviews*, *143*, 147–160, doi:10.1016/j.earscirev.2015.02.002.

Poeppl, R. E., and A. J. Parsons (2018), The geomorphic cell: a basis for studying connectivity, *Earth Surface Processes and Landforms*, *43*(5), 1155–1159, doi: 10.1002/esp.4300.

Poizot, E., Y. Mear, M. Thomas, and S. Garnaud (2006), The application of geostatistics in defining the characteristic distance for grain size trend analysis, *Computers and Geosciences*, *32*(3), 360–370, doi:10.1016/j.cageo.2005.06.023.

Poizot, E., Y. Mear, and L. Biscara (2008), Sediment Trend Analysis through the variation of granulometric parameters: A review of theories and applications, *Earth-Science Reviews*, *86*(1-4), 15–41, doi:10.1016/j.earscirev.2007.07.004.

Ranasinghe, R., T. M. Duong, S. Uhlenbrook, D. Roelvink, and M. J. F. Stive (2012), Climate-change impact assessment for inlet-interrupted coastlines, *Nature Climate Change*, *3*(1), 83–87, doi:10.1038/nclimate1664.

Read, J. M., K. T. Eames, and W. J. Edmunds (2008), Dynamic social networks and the implications for the spread of infectious disease, *Journal of the Royal Society Interface*, *5*(26), 1001–1007, doi:10.1098/rsif.2008.0013.

Reimann, T., P. D. Notenboom, M. A. de Schipper, and J. Wallinga (2015), Testing for sufficient signal resetting during sediment transport using a polymineral multiple-signal luminescence approach, *Quaternary Geochronology*, *25*, 26–36, doi:10.1016/j.quageo.2014.09.002.

Rijkswaterstaat (1999), *Sedimentatlas Waddenzee*, 36–38 pp., Rijkswaterstaat, Haren, Netherlands.

Rijkswaterstaat (2016), Vaklodingen Dataset.

Roelvink, J. (2015), Addressing Local And Global Sediment Imbalances: Coastal Sediments As Rare Minerals, in *Coastal Sediments 2015*, pp. 1–13, San Diego, CA.

Rogers, J. S., S. G. Monismith, O. B. Fringer, D. A. Koweek, and R. B. Dunbar (2016), A coupled wave-hydrodynamic model of an atoll with high friction: mechanisms for flow, connectivity, and ecological implications, *Ocean Modelling*, *0*, 1–17, doi:10.1016/j.ocemod.2016.12.012.

Rosenbauer, R. J., A. C. Foxgrover, J. R. Hein, and P. W. Swarzenski (2013), A Sr-Nd isotopic study of sand-sized sediment provenance and transport for the San Francisco Bay coastal system, *Marine Geology*, *345*, 143–153, doi:

10.1016/j.margeo.2013.01.002.

Rossi, V., E. Ser-Giacomi, C. Lõpez, and E. Hernández-García (2014), Hydrodynamic provinces and oceanic connectivity from a transport network help designing marine reserves, *Geophysical Research Letters*, *41*(8), 2883–2891, doi: 10.1002/2014GL059540.

Rubinov, M., and O. Sporns (2010), Complex network measures of brain connectivity: Uses and interpretations, *NeuroImage*, *52*(3), 1059–1069, doi: 10.1016/j.neuroimage.2009.10.003.

Ruggiero, P., G. M. Kaminsky, G. Gelfenbaum, and N. Cohn (2016), Morphodynamics of prograding beaches: A synthesis of seasonal- to century-scale observations of the Columbia River littoral cell, *Marine Geology*, *376*, 51–68, doi: 10.1016/j.margeo.2016.03.012.

Scott, J. (2011), Social network analysis : developments , advances , and prospects, pp. 21–26, doi:10.1007/s13278-010-0012-6.

Sexton, W. J., and M. O. Hayes (1983), Natural Bar-Bypassing of Sand at a Tidal Inlet, in *Proceedings of the Coastal Engineering Conference*, vol. 2, pp. 1479–1495, doi:10.9753/icce.v18.90.

Sha, L. P. (1989), Sand transport patterns in the ebb-tidal delta off Texel Inlet, Wadden Sea, The Netherlands, *Marine Geology*, *86*, 137–154, doi:10.1016/0025-3227(89)90046-7.

Smith, J. B., and D. M. FitzGerald (1994), Sediment transport patterns at the Essex River Inlet ebb-tidal delta, Massachusetts, U.S.A. , *Journal of Coastal Research*, *10*(3), 752–774.

Son, C. S., B. W. Flemming, and A. Bartholomä (2011), Evidence for sediment recirculation on an ebb-tidal delta of the East Frisian barrier-island system, southern North Sea, *Geo-Marine Letters*, *31*(2), 87–100, doi:10.1007/s00367-010-0217-8.

Soulsby, R. L., C. T. Mead, B. R. Wild, and M. J. Wood (2011), Lagrangian model for simulating the dispersal of sand-sized particles in coastal waters, *Journal of Waterway, Port, Coastal and Ocean Engineering*, *137*(3), 123–131, doi: 10.1061/(ASCE)WW.1943-5460.0000074.

Sperry, M. M., Q. K. Telesford, F. Klimm, and D. S. Bassett (2017), Rentian scaling for the measurement of optimal embedding of complex networks into physical space, *Journal of Complex Networks*, *5*(2), 199–218, doi:10.1093/comnet/cnw010.

Stive, M., M. Capobianco, Z. Wang, P. Ruol, and M. Buijsman (1998), Morphodynamics of a tidal lagoon and the adjacent coast, in *Eighth International Biennial Conference on Physics of Estuaries and Coastal Seas, September 1996*, pp. 397–407, The Hague, The Netherlands.

Stive, M. J. F., and Z. B. Wang (2003), Morphodynamic modeling of tidal basins and coastal inlets, *Elsevier Oceanography Series*, *67*(C), 367–392, doi: 10.1016/S0422-9894(03)80130-7.

Stive, M. J. F., M. A. de Schipper, A. P. Luijendijk, R. Ranasinghe, J. van Thiel de Vries, S. G. J. Aarninkhof, C. van Gelder-Maas, S. de Vries, M. Henriquez, and S. Marx (2013), The Sand Engine: A solution for vulnerable deltas in the 21st century?, in *Coastal Dynamics 2013*, pp. 1537–1546.

Storlazzi, C. D., M. van Ormondt, Y.-L. Chen, and E. P. L. Elias (2017), Modeling Fine-Scale Coral Larval Dispersal and Interisland Connectivity to Help Designate Mutually-Supporting Coral Reef Marine Protected Areas: Insights from Maui Nui, Hawaii, *Frontiers in Marine Science*, *4*(December), 1–14, doi: 10.3389/fmars.2017.00381.

Tejedor, A., A. Longjas, I. Zaliapin, and E. Foufoula-Georgiou (2015a), Delta channel networks: 1. A graph-theoretic approach for studying connectivity and steady state transport on deltaic surfaces, *Water Resources Research*, *51*(6), 3998–4018, doi:10.1002/2014WR016577.

Tejedor, A., A. Longjas, I. Zaliapin, and E. Foufoula-Georgiou (2015b), Delta channel networks: 2. Metrics of topologic and dynamic complexity for delta comparison, physical inference, and vulnerability assessment, *Water Resources Research*, *51*(6), 4019–4045, doi:10.1002/2014WR016604.

Tejedor, A., A. Longjas, R. Caldwell, D. A. Edmonds, I. Zaliapin, and E. Foufoula-Georgiou (2016), Quantifying the signature of sediment composition on the topologic and dynamic complexity of river delta channel networks and inferences toward delta classification, *Geophysical Research Letters*, *43*(7), 3280–3287, doi: 10.1002/2016GL068210.

Tejedor, A., A. Longjas, D. A. Edmonds, I. Zaliapin, T. T. Georgiou, A. Rinaldo, and E. Foufoula-Georgiou (2017), Entropy and optimality in river deltas, *Proceedings of the National Academy of Sciences*, *114*(44), 11,651–11,656, doi: 10.1073/pnas.1708404114.

Treml, E. A., P. N. Halpin, D. L. Urban, and L. F. Pratson (2008), Modeling population connectivity by ocean currents, a graph-theoretic approach for marine conservation, *Landscape Ecology*, *23*(S1), 19–36, doi:10.1007/s10980-007-9138-y.

Turnbull, L., K. Tockner, R. Poeppl, M.-t. Hütt, S. Keesstra, L. J. Bracken, A. J. Parsons, S. Kininmonth, R. Masselink, L. Liu, and A. A. Ioannides (2018), Connectivity and complex systems: learning from a multi-disciplinary perspective, *Applied Network Science*, *3*(1), doi:10.1007/s41109-018-0067-2.

Urban, D. L., E. S. Minor, E. A. Treml, and R. S. Schick (2009), Graph models of habitat mosaics, *Ecology Letters*, *12*(3), 260–273, doi:10.1111/j.1461-0248.2008.01271.x.

Van Der Wegen, M., A. Dastgheib, B. E. Jaffe, and D. Roelvink (2011), Bed composition generation for morphodynamic modeling: Case study of San Pablo Bay in California, USA, in *Ocean Dynamics*, vol. 61, pp. 173–186, doi:10.1007/s10236-010-0314-2.

van Sebille, E., S. M. Griffies, R. Abernathey, T. P. Adams, P. Berloff, A. Biastoch, B. Blanke, E. P. Chassignet, Y. Cheng, C. J. Cotter, E. Deleersnijder, K. Döös, H. F. Drake, S. Drijfhout, S. F. Gary, A. W. Heemink, J. Kjellsson, I. M. Koszalka, M. Lange, C. Lique, G. A. MacGilchrist, R. Marsh, C. G. Mayorga Adame, R. McAdam, F. Nencioli, C. B. Paris, M. D. Piggott, J. A. Polton, S. Rühs, S. H. Shah, M. D. Thomas, J. Wang, P. J. Wolfram, L. Zanna, and J. D. Zika (2018), Lagrangian ocean analysis: Fundamentals and practices, *Ocean Modelling*, *121*(October 2017), 49–75, doi:10.1016/j.ocemod.2017.11.008.

Van Weerdenburg, R. J. (2019), Exploring the relative importance of wind for exchange processes around a tidal inlet system: the case of Ameland Inlet, Master's thesis, Delft University of Technology.

Van Wesenbeeck, B. K., J. P. Mulder, M. Marchand, D. J. Reed, M. B. De Vries, H. J. De Vriend, and P. M. Herman (2014), Damming deltas: A practice of the past? Towards nature-based flood defenses, *Estuarine, Coastal and Shelf Science*, *140*, 1–6, doi:10.1016/j.ecss.2013.12.031.

Velegrakis, A. F., M. B. Collins, A. C. Bastos, D. Paphitis, and A. Brampton (2007), Seabed sediment transport pathway investigations: review of scientific approach and methodologies, *Geological Society, London, Special Publications*, *274*(1), 127–146, doi:10.1144/GSL.SP.2007.274.01.13.

Vitousek, S., P. L. Barnard, and P. Limber (2017), Can beaches survive climate change?, *Journal of Geophysical Research: Earth Surface*, *122*(4), 1060–1067, doi:10.1002/2017JF004308.

Vos, K., M. D. Harley, K. D. Splinter, J. A. Simmons, and I. L. Turner (2019), Sub-annual to multi-decadal shoreline variability from publicly available satellite imagery, *Coastal Engineering*, *150*(November 2018), 160–174, doi: 10.1016/j.coastaleng.2019.04.004.

Wang, Y., Q. Yu, J. Jiao, P. K. Tonnon, Z. B. Wang, and S. Gao (2016), Coupling bedform roughness and sediment grain-size sorting in modelling of tidal inlet incision, *Marine Geology*, *381*(September), 128–141, doi: 10.1016/j.margeo.2016.09.004.

Wang, Z. B., D. S. Van Maren, P. X. Ding, S. L. Yang, B. C. van Prooijen, P. de Vet, J. Winterwerp, H. J. De Vriend, M. J. F. Stive, and Q. He (2015), Human impacts on morphodynamic thresholds in estuarine systems, *Continental Shelf Research*, *111*, 174–183, doi:10.1016/j.csr.2015.08.009.

Wang, Z. B., E. P. Elias, A. J. van der Spek, and Q. J. Lodder (2018), Sediment budget and morphological development of the Dutch Wadden Sea: impact of accelerated sea-level rise and subsidence until 2100, *Netherlands Journal of Geosciences*, *97*(03), 183–214, doi:10.1017/njg.2018.8.

Wohl, E., G. Brierley, D. Cadol, T. J. Coulthard, T. Covino, K. A. Fryirs, G. Grant, R. G. Hilton, S. N. Lane, F. J. Magilligan, K. M. Meitzen, P. Passalacqua, R. E. Poeppl, S. L. Rathburn, and L. S. Sklar (2019), Connectivity as an emergent property of geomorphic systems, *Earth Surface Processes and Landforms*, *44*(1), 4–26, doi:10.1002/esp.4434.

Wong, F. L., D. L. Woodrow, and M. McGann (2013), Heavy mineral analysis for assessing the provenance of sandy sediment in the San Francisco Bay Coastal System, *Marine Geology*, *345*, 170–180, doi:10.1016/j.margeo.2013.05.012.